

Performance Analysis of MAC Protocols for Wireless Sensor Networks

by

Haoling Ma

B.Eng, Southeast University, 1992

A Thesis Submitted in Partial Fulfillment of the
Requirements for the Degree of

MASTER OF APPLIED SCIENCE

in the Department of Electrical and Computer Engineering

©Haoling Ma, 2009
University of Victoria

All rights reserved. This thesis may not be reproduced in whole or in part, by
photocopy or other means, without the permission of the author.

Performance Analysis of MAC Protocols for Wireless Sensor Networks

by

Haoling Ma

B.Eng, Southeast University, 1992

Supervisory Committee

Dr. Lin Cai, Supervisor
(Department of Electrical and Computer Engineering)

Dr. Xiao-Dai Dong, Department Member
(Department of Electrical and Computer Engineering)

Dr. Kui Wu, Outside Member
(Department of Computer Science)

Supervisory Committee

Dr. Lin Cai, Supervisor
(Department of Electrical and Computer Engineering)

Dr. Xiao-Dai Dong, Department Member
(Department of Electrical and Computer Engineering)

Dr. Kui Wu, Outside Member
(Department of Computer Science)

Abstract

A sensor network is comprised of a large number of sensor nodes with limited power, which collect and process data from a target domain and transmit information back to specific sites, such as, headquarters and disaster control centers. Since the wireless communication channel shared by sensor nodes is broadcast in nature, a Medium Access Control (MAC) protocol is needed to specify how nodes share the channel, which plays a central role in the performance of a sensor network.

In this thesis, we investigate the performance of randomized and time hopping Aloha MAC protocols by theoretical analysis and simulations. The first part of our research formulates the multiple access collision problem raised from the ARGOS satellite telemetry system. We analyze the factors that affect the performance of the system and derive the mathematical model. We simulate the system and generate valuable performance results for design purpose. In the second part of the thesis, we extend our research to sensor networks with Impulse Radio Ultra WideBand (IR-UWB) physical layer defined in IEEE802.15.4a. We analyze and model the time

hopping Aloha MAC protocol and verify the results with simulations using NS-2 network simulator.

Table of Contents

Supervisory Committee	i
Abstract	iii
Table of Contents	v
List of Tables	viii
List of Figures	ix
List of Abbreviations	xi
List of Symbols	xiii
Acknowledgment	xiv
Dedication	xv
1 Introduction	1
1.1 MAC Protocol Overview	2
1.2 Motivations and Problem Formulation	5
1.3 Contributions	6
1.4 Thesis Organization	7
2 Performance Analysis of Randomized MAC Scheme for Satellite Telemetry Systems	9
2.1 Architecture and Air Interface of Argos System	11
2.1.1 System Architecture	11
2.1.2 Air Interface	13

2.1.3	Randomized Transmission Scheme	15
2.2	Performance Analysis	16
2.2.1	Success Probability	17
2.2.2	Success Probability with Randomized Transmission Scheme	19
2.2.3	Numerical Results	20
2.3	Conclusion	25
3	Performance Analysis of TH IR-UWB with Aloha MAC Protocol	26
3.1	IR-UWB Fundamentals	27
3.2	IEEE802.15.4a Standard	29
3.3	Impulse UWB Radio and Multiple User Interference	33
3.4	Related Works on UWB MAC Design and Performance Analysis	37
3.5	Performance Analysis of TH Aloha	41
4	Numerical Results and Performance Evaluation by Simulation	44
4.1	Numerical Results of Analysis	44
4.1.1	Throughput vs. offered load	46
4.1.2	Impact of Packet Size on Throughput	47
4.2	Analysis Validation	47
4.3	Performance Study by Simulations	47
4.3.1	Network Performance of Symmetric Topology	51
4.3.2	Simulation of Random Topology	52
4.3.3	Impact of Frame Size on Throughput	55
4.3.4	Impact of Node Density on Network Throughput	57
4.3.5	Successful Packet Delivery Rate	58
5	Conclusion and future work	61
5.1	Conclusions and Summary of Contributions	61

5.2	Limitations and Further Work	62
	Bibliography	64
A	ARGOS System Aloha Simulation Programs	70

List of Tables

3.1	UWB spectrum mask for indoor and outdoor data communications [1]	28
3.2	UWB PHY channel number and frequencies [2]	30
4.1	Numerical example parameters	45
4.2	Simulation parameters	50

List of Figures

2.1	Argos avian backpack PTT transmitter [3]	12
2.2	Frequency allocation of Argos-2 system [4]	14
2.3	Air interface of Argos-2	14
2.4	Deterministic transmission scheme(a) vs randomized transmission scheme(b)	16
2.5	Success possibility vs number of users with deterministic transmission scheme	18
2.6	Success probability vs number of nodes	21
2.7	Success probability vs random level and number of user(random level 0.05)	22
2.8	Maximum user numbers vs random level and success probability . . .	23
2.9	Success probability vs number of users under random level 0.1 and 0.05	24
3.1	IR-UWB PHY symbol structure [2]	31
3.2	Diagram of number of interfering nodes(N_{int}) with time for Aloha . .	35
3.3	IR-UWB symbol state	42
4.1	TH UWB Aloha throughput	46
4.2	Impact of packet size on aggregate throughput	48
4.3	Normalized throughput vs offered load, analysis vs simulation. Packet size=128 bytes. Simulation with 7 Tx and Rx pairs, line up topology.	49
4.4	Aggregate throughput as a function of number of nodes in a symmetric topology scenario. TH Aloha, Single data link layer data rate R= 10.2 kbps, $20m \times 20m$ area, inter-packet interval 0.1 second)	52

4.5	Normalized throughput vs number of nodes. Packet size=128 bytes, symmetric topology scenario. TH Aloha, Single data link layer data rate $R= 10.2$ kbps, $20m \times 20m$ area, inter-packet interval 0.1 second	53
4.6	Average delay vs number of nodes. Packet size=128 bytes, symmetric topology scenario. TH Aloha, Single data link layer data rate $R= 10.2$ kbps, $20m \times 20m$ area, inter-packet interval 0.1 second	54
4.7	Aggregate throughput as a function of number of nodes. Random topology and symmetric topology, TH Aloha, $20m \times 20m$ area, Single data link layer data rate $R= 10.2$ kbps, inter-packet interval 0.1 second	55
4.8	Normalized throughput vs number of nodes. Random topology and symmetric topology, TH Aloha, $20m \times 20m$ area, Single data link layer data rate $R= 10.2$ kbps, inter-packet interval 0.1 second	56
4.9	Average delay vs number of nodes. Random topology and symmetric topology, TH Aloha, $20m \times 20m$ area, Single data link layer data rate $R= 10.2$ kbps, inter-packet interval 0.1 second	57
4.10	Normalized throughput affected by packet size. Random topology, TH Aloha, $20m \times 20m$ area, inter-packet interval 0.1 second	58
4.11	Aggregate network throughput affected by nodes density. Random topology and symmetric topology, TH Aloha, $20m \times 20m$ and $40m \times 40m$ area, Single data link layer data rate $R= 10.2$ kbps, inter-packet interval 0.1 second	59
4.12	Successful packet delivery rate. Nodes are randomly placed in an area $20m \times 20m$, average transmission interval is 0.1 seconds)	60

List of Abbreviations

ACK	Acknowledgment
BER	Bit error rate
BO	Backoff
BPM	Burst position modulation
bps	Bits per second
BPSK	Binary phase shift keying
BPM-BPSK	Burst position modulation and binary phase shift keying
CBR	Constant Bit Rate
CCA	Clear channel assessment
CD	Collision Detection
CDMA	Code Division Multiple Access
CSMA	Carrier Sense Multiple Access
CSMA/CA	Carrier Sense Multiple Access with Collision Avoidance
CSS	Chirp spreading sequence
DATA	Data packet
DSP	Digital Signal Processing
EIRP	Equivalent Isotropically Radiated Power
FCC	Federal Communication Commission
FEC	Forward error correction
FDMA	Frequency Division Multiple Access
FTP	File Transfer Protocol
GHz	Gigahertz
GPS	Global Positioning System
Gbps	Gigabit per second
HTTP	Hyper Text Transfer Protocol

IEEE	Institute of Electrical and Electronics Engineers
IR	Impulse Radio
ISO	International Organization for Standardization
MAC	Medium Access Control
Mbps	Megabit per second
MHz	Megahertz
OFDM	Orthogonal frequency-division multiplexing
OSI	Open System Interconnect model
PHR	PHY header
PHY	Physical layer
PMT	Platform Messaging Transceiver
PPM	Pulse position modulation
PRF	Pulse repetition frequency
PSDU	PHY service data unit
PTT	Platform Transmitter Terminal
RF	Radio frequency
RTS	Request to send
SHR	Synchronization header
SINR	Signal to Interference plus Noise ratio
SNR	Signal to Noise Ratio
TDMA	Time Division Multiple Access
TH	Time hopping
UWB	Ultra-Wideband technology
WLAN	Wireless local area network
WPAN	Wireless personal area network
WSN	Wireless Sensor Networks

List of Symbols

f_c	Center frequency
F_{ch}	Number of uplink channels
L_r	Random level of the transmission interval
$h^{(k)}$	Burst hopping sequence
N	Number of active users in the footprint of a satellite
N_{burst}	Burst positions per symbol
N_{cpb}	UWB pulses per burst
N_{hop}	Number of hopping positions
$P_{success}$	The probability that a satellite successful receives a message
R	Average transmission interval determined
R_r	Randomized transmission interval
R_{sym}	Symbol rate
$s_{n+kN_{cpb}}$	The scrambling sequence
T_b	Transmission time of a message
T_{burst}	Burst duration
T_c	UWB pulse width
T_{dsym}	Symbol duration
T_p	Duration time of a pass
W	Bandwidth

Acknowledgment

I would like to express my deep appreciation for the invaluable advice, continuous support and adequate patience I have received from my supervisor, Dr. Lin Cai. The research and thesis could never been completed without her precious advice and encouragement. I also want to give my gratitude to Dr. Xiaodai Dong and Dr. Kui Wu for their participation in my committee and their help during my study.

Next, I would like to give my thanks to all the members in our Communication and Networking Group, namely: Fengdan Wang, Ruonan Zhang, Emad Shihab, Deer Li, Ahmad Ali Abdullah, and Dr. Jianping Pan. I appreciate the time and experiences that you shared with me.

Special thanks to Dr. Jeff Goodyear, many of my research interests were inspired by conversations with him. I also want to give my thanks to all my colleagues at HABIT Research and Millimeter Wave Lab of National Research Council HIA. Thank you for your encouragement and support all the way through my study.

Most importantly, I will not complete or even start my study without the support from my wife Zihan, my son Jingan and my parents. It is impossible for me to reach this step without your love, sacrifice and understanding.

Dedication

To my family

Chapter 1

Introduction

Wireless Sensor Networks (WSNs) have attracted many research interests from both industry and academia in the past decade. There are growing interests which are driven by various perspective areas of applications, such as environmental study, ocean research, health care, home automation and military [5]. These applications bring also some interesting research challenges across all layers of the network protocols.

As wireless medium is open and shared, any terminals may access to it at any time. A channel access method or multiple access method is required to allow several terminals connected to the same physical medium to transmit over it and to share its capacity. Such multiple access and control mechanisms are defined in media access control (MAC) protocols [6], which are provided by the data link layer in the OSI model and the link layer of the TCP/IP model. MAC protocols defined rules to force terminals to access the wireless medium in an orderly and efficient manner. In general, a MAC protocol should be able to efficiently regulate/coordinate users sharing the medium and achieve the following objectives [7]:

- Efficiency: The network resources can be efficiently utilized.
- Fairness: Every user has a fair share of the medium.

- Robustness: The tolerance of interference, errors and device failures.
- Stability: The network will not be driven to congestion collapse.
- Limited delay: Users should experience a bounded delay.
- Scalability: The MAC protocol should scale well to a growing number of users.
- Low power consumption: Energy consumption to the users should be relatively low, as terminals are battery powered.

1.1 MAC Protocol Overview

We use the TCP/IP reference model used in the Internet to elaborate the functions of MAC protocols. The TCP/IP reference model specifies five layers: application, transport, network, link, and PHY layers [6]. The top layer is the application layer, which is designed to support different applications, such as Hyper Text Transfer Protocol (HTTP) for web. Below the application layer is the transport layer, which hides the underlying network impairment from the application layer and provides end-to-end datagram transmission services. The network layer routes the data from the source to the destination. The link layer provides a point-to-point connection service between two communicating nodes and it may conceal the impairments of the physical medium from the upper layers. The link layer also provides medium access control which will be the focus of this thesis. The bottom layer, the physical layer, is designed to transmit bit streams over a communication channel.

A MAC protocol coordinates the terminals in a network and resolves the contention among their accessing to the shared medium. With a shared communication channel, a properly designed MAC protocol is the key to the desired system performance such as high throughput and low delay. MAC protocols can

be categorized as centralized or distributed, depending on their control methods [8]. Centralized MAC protocols require base stations to control the network activities, which is not feasible in most wireless sensor networks applications, whereas distributed MAC protocols are simple to implement, scalable, and robust.

A multiple access method is based on a multiplex method, that allows several data streams or signals to share the same communication channel or physical media [6]. MAC protocols can also be divided into three categories according to their multiple access techniques: static, random and hybrid access [9].

Static access MAC protocols allocate the resources deterministically between users, such as:

- Time Division Multiple Access (TDMA), where time is slotted and different time slots are allocated to different users;
- Frequency Division Multiple Access (FDMA), where frequency band is divided into frequency channels, and several users can simultaneously transmit using different frequency channels;
- Spread spectrum multiple access. For example, using the Code Division Multiple Access (CDMA) technology, users transmit simultaneously at the same frequency, but each user uses a different code. Codes are orthogonal or pseudo-random to minimize the interference to each other. CDMA technologies are widely used in the third generation mobile communication systems [10].

Previous studies indicated that static MAC protocols can provide a certain level of QoS due to dedicated resource allocation, but the utilization efficiency is low with burst traffic. Static MAC protocols usually need infrastructure for centralized control, which is also a disadvantage for WSNs [11].

In random access protocols, users compete to access the medium without guarantee that the transmission will be successful. The most popular random access protocols are:

- Aloha [12]. It is widely used in satellite WSNs. Users may attempt to transmit randomly and may suffer collisions. Retransmission or repeated attempt is necessary to assure the successful transmission.
- Carrier Sense Multiple Access (CSMA). With CSMA, users first sense the channel before transmitting. If the channel is busy, the transmission is delayed. There are other techniques combined with CSMA, such as Collision Detection (CD) and Collision Avoidance (CA).

The main advantage of a random access protocol is that it does not require a central controller, which implies relatively simple implementation; the disadvantages are inevitable channel idle periods and frame collisions, which waste the channel bandwidth.

Hybrid access protocols combine the advantages of the random access and guaranteed access protocols to achieve flexibility, efficiency and QoS. Access protocols of 3G cellular networks are examples of combination of random access and static access [13]. A user initiates a communication link by accessing the base station with a random access protocol. If the initiation is successful, the user will be assigned dedicated time slots or a code until it intends to end the communication.

The incorporation of random access and other multiplexing mechanisms provides more flexibility for network applications. It is worthwhile to investigate the performance of such hybrid protocols. In this thesis, we first investigate the MAC protocols of ARGOS system, which is a combination of Aloha random access and FDMA. We formulate the system performance and study a randomized scheme proposed to solve the periodical transmission collision problem. In the second part of

our research, we analyze and simulate the time hopping Aloha Medium Access Control (MAC) protocol used for IR-UWB (Impulse Radio Ultra Wide band) physical layer, which is defined in the IEEE802.15.4a standard [2]. The analysis and simulation results indicate that Aloha protocol performs quite well with TH IR-UWB physical layer under medium and light load. Simultaneous transmission is achievable and can achieve significant performance gain.

There are already a lot of MAC protocols proposed for WSNs in the literature. Excellent reviews can be found in [14] and [15]. The extreme application environments of WSN post some constraints on MAC protocol design. These constraints include low power consumption, low cost, small size and high reliability. Wireless sensor nodes are usually deployed in remote areas or floating in water. They are powered by batteries and deployed in large amount. These factors need to be carefully treated to design a successful network.

Based on the above constraints, there are some special requirements on the design of MAC protocols of wireless sensor networks, as listed below:

- Simplicity, to reduce power consumption and less requirement on hardware;
- Robustness, to reduce the requirement of repairing and maintenance, working under interference and extreme conditions;
- Distributed, to improve the network reliability and robustness.

1.2 Motivations and Problem Formulation

Performance study of wireless sensor network MAC protocols with analytical modeling and simulation is helpful for researchers and industry to understand the complex relationships among protocol parameters, find the bottleneck and improve the protocol performance during network design. The research objective of this thesis

is to solve two MAC performance related problems with the Aloha protocol. One is from an industry application - ARGOS satellite telemetry system, and the other one is on Time Hopping (TH) Aloha with IR-UWB physical layer.

Our interest of studying the multi-channel Aloha MAC protocol originated from a transmission collision problem observed with the ARGOS satellite telemetry system. The ARGOS system is an infrastructure based, single-hop satellite network. The ground terminals of the ARGOS system, Platform Transmitter Terminal (PTT), transmit temperature, pressure and other data to the satellite [16]. When the density of terminals increases, the possibility of transmission collisions will increase dramatically. Transmissions from some terminals overlap with each other periodically and totally loss function. The same problem occurs in another system used to track patients with the Alzheimer's disease [17]. When the number of terminals with the same frequency increases in the same receiving area, transmitted pulses collide with each other and cannot be retrieved by receivers.

We then extend our research to MAC protocol defined in the IEEE 802.15.4a standard, which combines Aloha with CDMA spreading coding [2]. The 802.15.4a version 2007 introduced new PHY alternatives, chirp spreading sequence (CSS) working in 2.4GHz ISM band and UWB PHY in sub-GHz, low UWB band and high UWB band. The standard also defined an optional MAC layer random access scheme adapted to the UWB PHY layer. This distributed light-weighted random protocol will simplify the design and implementation of network terminal devices, but collision losses need to be considered due to the nature of random access.

1.3 Contributions

In this thesis, we analytically study the performance of the MAC protocols used by a satellite WSN. We also propose how to improve the MAC protocol used. The

effectiveness of the proposed scheme is validated by simulations. The system's successful transmission rate is improved under heavy load. The improved MAC scheme was implemented on a small scale bird flu monitoring network with about 200 wireless terminals. This network achieved an above 95% successful transmission rate.

Our second main contribution is the performance evaluation of time hopping random access MAC protocol with IR-UWB physical layer by both analysis and simulation. We study the throughput performance affected by different network and wireless transmission parameters, and indicate how these parameters affect the overall throughput. Our results also demonstrate that the time hopping Aloha MAC protocol performs well together with IR-UWB, which has a significant improvement on aggregate network throughput compared to pure Aloha and slotted Aloha, especially under medium and heavy load.

1.4 Thesis Organization

In Chapter 2, we give a brief introduction of ARGOS satellite telemetry system, and present the Aloha protocol with a randomized transmission strategy. We model the system throughput and verify our analysis with simulation written in C language. The effects of different factors on the system performance are also presented.

The analytical model used to study the performance of Aloha MAC protocol with IR-UWB physical layer is presented in Chapter 3. First, we have a brief literature review on the research work related to IR-UWB MAC protocols and present the technology challenges. Then, we derive the aggregate network throughput. Analysis of the effect of packet size and number of users on the aggregate throughput is presented.

In Chapter 4, we first validate the analysis of the Aloha MAC protocol with IR-UWB physical layer by simulations with NS-2. We then evaluate the network performance, and how packet size and density of terminals affect the aggregate network throughput with extensive NS-2 simulations.

Chapter 5 concludes the contributions of our research and also points out the limitations that can be further improved in future works.

Chapter 2

Performance Analysis of Randomized MAC Scheme for Satellite Telemetry Systems

Satellite and radio telemetry systems are widely used in environment research. On February 16, 2005, 61 countries agreed to establish Global Earth Observation System of Systems (GEOSS), which will revolutionize the understanding of Earth over the following ten years [4]. Nearly 40 international organizations also support this agreement. This agreement will help all nations involved produce and manage their information in a way that benefits the environment. The Argos system is one of the most popular telemetry systems worldwide, which is dedicated to Earth observation, scientific and environmental research. It has an excellent track record for data collection, processing and dissemination to the scientific and international community. It offers a robust and proven tool for understanding environmental factors. The Argos system fits perfectly into the framework defined by the emerging Global Earth Observation System of Systems [18]. In the last thirty years, the Argos system has migrated with three generations: Argos 1, 2, and 3 [19].

With the popularity of the Argos system, more and more devices will share and compete for the premium uplink satellite communication bandwidth. Since Aloha MAC protocol is adopted in Argos system, the number of devices is limited to maintain reasonable performance [6]. If the number of devices in an area exceeds certain limit, most transmissions may fail due to collisions, and many nodes become “dead nodes” so that no messages can be received from them for a while. To mitigate the “dead node” problem and ensure the effectiveness and efficiency of the system, the maximum number of users in an area should be quantified to allow appropriate control of the density of users. This is the main motivation of our research in this chapter.

The analysis of Aloha found in literature is based on the assumptions that nodes are transmitting independently and randomly. The data traffic in the system is a random variable and follows Poission distribution [6]. However, in some network applications, especially wireless sensor networks, the periodical readings from specific sensors are expected. Transmissions are required in a periodical manner rather than totally random.

The main contributions of this chapter are as follows. First, we addressed the periodical transmission collisions problem happened between Argos transmitters, which results in the long term missing of certain transmitters. We quantify the probability of successful reception in the Argos system and the system capacity, i.e., the maximum number of users that can be supported in an area with guaranteed success rate. Then, we analyzed the performance of the randomized transmission scheme, which has not been found in literature. The randomized scheme itself is simple to implement, and it can also significantly improve the system capacity.

The remainder of this chapter is organized as follows. In Section 2.1, We briefly introduce the architecture of the Argos system and its air interface, explained the concept and terminology to formulate the system. We identify the periodical

transmission congestion problem of the existing system, which uses a deterministic transmission pattern. A randomized transmission scheme is then introduced to improve the system performance.

In Section 2.2, to evaluate the effectiveness of the randomized scheme, we obtain the theoretical capacity of the system with and without the randomized transmission scheme. The analytical results show the significance of the randomized scheme. Concluding remarks are presented in Section 2.3.

2.1 Architecture and Air Interface of Argos System

2.1.1 System Architecture

The Argos system has three interactive subsystems [20].

- User devices: Platform Transmitter Terminals (PTTs) for the first and second generation Argos system, Platform Messaging Transceiver (PMT) for the third generation [19];
- The Space Segment;
- The Ground Segment.

User Devices

Argos operation begins with transmissions from PTTs and PMTs attached to sensor equipment and the platform from which data is collected. The difference between PTTs and PMTs is that PTTs only have transmitters, whereas, PMTs have both transmitters and receivers. Fig. 2.1 is a picture of a PTT transmitter. PTTs and PMTs have been adopted for applications such as tracking migratory birds, monitoring ice floes in harsh environments, etc. They are configured by size, weight,



Figure 2.1: Argos avian backpack PTT transmitter [3]

power consumption, and housing according to applications. The smallest PTTs, used to track birds, weigh as 10.2 grams unpotted and 25 grams finished modules with battery [3]. By setting the proper duty cycle and repetition rate, a single AA Lithium cell can operate a year or more. With combined Lithium and solar battery, even more operation time can be achieved [3].

The Space Segment

Argos instruments are flown on board the National Oceanic and Atmospheric Administration (NOAA) Polar Orbiting Environmental Satellites (POES) and Metop satellite from European Meteorological Satellite organization (Eumetsat) [4]. The Argos satellites orbit the earth in near-polar, sun-synchronous orbits. They can see the North and South Poles on each orbital revolution. Each satellite passes within visibility of any given transmitter at almost the same local solar time each day. The time required to complete one revolution around the Earth is approximately 102 minutes. Because of the near-polar orbit, the number of daily passes over a

transmitter increases with latitude. At the poles, each satellite passes approximately 14 times a day for a total of 28 times (with two satellites). At the equator, there are totally 6 to 7 passes per day [16].

The Ground Segment

The ground segment comprises of three parts:

- ground antennas relay data from satellites to processing centers;
- processing centers collect all incoming data, process them and distribute them to customers;
- Argos users receive data or send command to their PMTs through world-wide web.

2.1.2 Air Interface

Frequency Allocation

PTTs and PMTs are all working on the same center frequency at 401.65 MHz. The bandwidth are 24, 80 and 110 KHz for Argos-1, Argos-2 and Argos-3, respectively. Because Argos-2 is the current system on duty, our analysis focuses on it. Our approach can be extended to other generations of Argos systems. The channel allocation of Argos-2 is illustrated in Fig. 2.2 [4].

Air Interface

PTTs in the ground segment transmit encoded messages at regular intervals. The interval is fixed according to the application, in a range between 45 s and 200 s. Transmission burst length is in the range of 360 ms to 920 ms, depending on the applications as well.

The duration window of a satellite visible to a transmitter is called a “pass”. It lasts between 8 and 15 minutes (with the average of 10 minutes). In this window

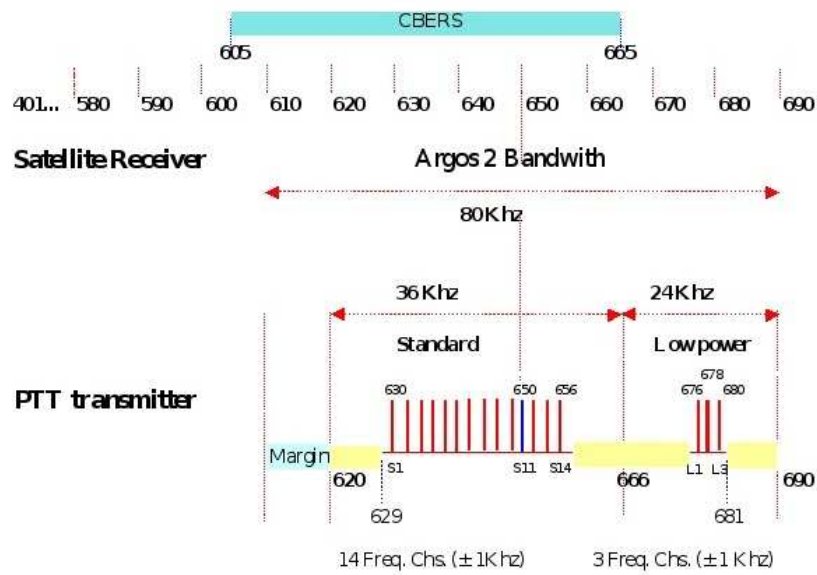


Figure 2.2: Frequency allocation of Argos-2 system [4]

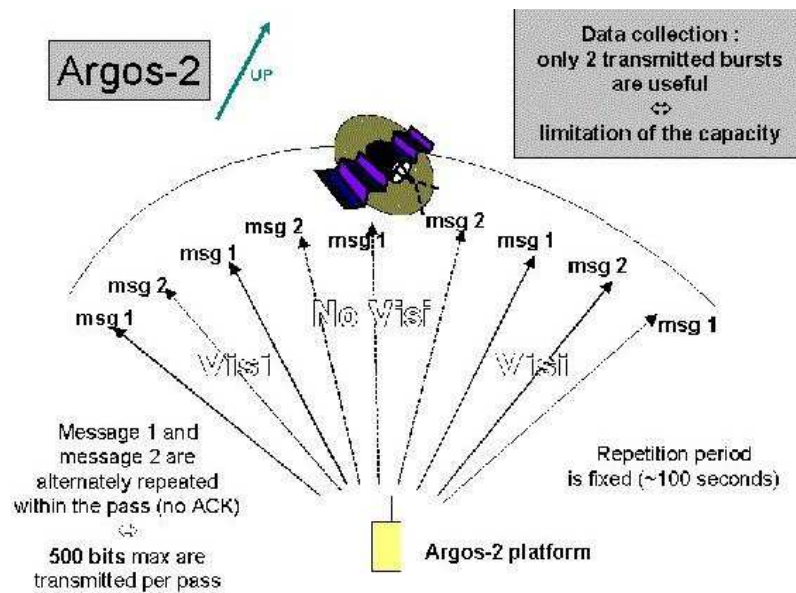


Figure 2.3: Air interface of Argos-2

of time, a receiver on board satellites can receive the transmissions of the customer terminals. The Argos-2 message transmitting scheme is shown in Fig. 2.3 [18]. The uplink has a number of channels at different frequencies. Each PTT will be initialized to use one of the channels randomly, and it will repeat transmissions at a constant rate during the pass of a satellite.

2.1.3 Randomized Transmission Scheme

Since the user devices of the Argos system should be simple and energy-conservative, these devices are equipped with transmitter only. Therefore, all carrier-sense based MAC protocols and resource allocation schemes are not applicable. They share the uplink satellite channel using the Aloha MAC protocol.

If two or more transmissions using the same frequency band overlap in time, collision occurs and all colliding transmissions are failed. If all of these devices transmit periodically, once the collision of the first attempt occurs, all the following retransmissions will fail due to collisions. To solve the problem, a randomized transmission scheme has been recommended by Argos recently [21], which will overcome the periodical overlapping problem that leads to low success rate and low system capacity.

The randomized transmission scheme let devices transmit in their repetition rate but with a random deviation, as shown in Fig. 2.4. To effectively reduce the correlation between consecutive transmissions during a satellite pass, random deviation is chosen to be uniformly distributed. Thus, the randomized transmission interval R_r is:

$$R_r = R(1 + L_r(X - 0.5)), \quad (2.1)$$

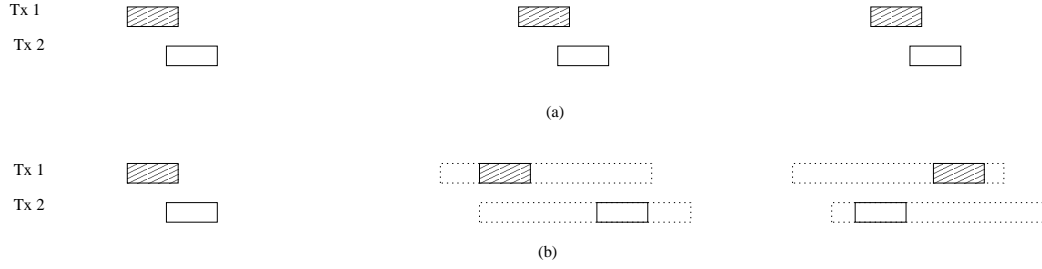


Figure 2.4: Deterministic transmission scheme(a) vs randomized transmission scheme(b)

where R is the average transmission interval determined by the Argos system, L_r is the random level of the transmission interval, choosing from 0 to 1, and X is a random variable uniformly distributed between 0 and 1. R is a constant assigned by Argos according to applications, e.g., R is set to 60 s for animal tracking, 100 s for ocean temperature monitoring.

In the following section, we will analyze the system performance with the deterministic and randomized transmission schemes, respectively.

2.2 Performance Analysis

We define the probability that the satellite successfully receives a copy of the message transmitted by a device during a satellite pass as P_{success} . It is determined by the following system parameters:

- N : number of active users in the footprint of a satellite;
- T_p : duration time of a pass;
- R : transmission interval;
- T_b : transmission time of a message;
- F_{ch} : number of uplink channels.

According to [19], the average pass duration, T_p , of an Argos satellite is 10 minutes. Transmission time of a message lasts from 360 ms to 920 ms. For Argos-2, there are 14 standard channels with 2 KHz bandwidth, and 3 low power channels, totally 17 channels. For Argos-3, a high data rate channel (4 KHz bandwidth) will be added.

In the following, we first investigate the successful reception probability during a pass, and the maximum number of user devices can be supported in the same footprint to guarantee the success rate of each device.

2.2.1 Success Probability

A PTT transmission can be successfully received by the satellite receiving unit if there is no other same-channel transmissions during its transmission time. Since there is no time-synchronization among users and the user devices may not be equipped with a receiver, the up-link medium access uses the pure Aloha protocol [6]. We assume that the messages have a constant frame size, and with a fixed transmission time T_b . For pure Aloha networks, the vulnerable time of a transmission is $2T_b$.

During a satellite pass, each device may start to transmit at different time, with the rate of one transmission per R . The probability that a PTT starts to transmit within any T_b interval is given as:

$$\tau = T_b/R \quad (2.2)$$

As defined before, T_b and R are the transmission time and the interval between consecutive transmissions. To estimate the value of τ , we use the average values of T_b and R , e.g., 500 ms and 100 s, respectively. The probability that a PTT transmits in a specific frequency channel in a T_b interval is:

$$p_c = \tau/F_{ch}. \quad (2.3)$$

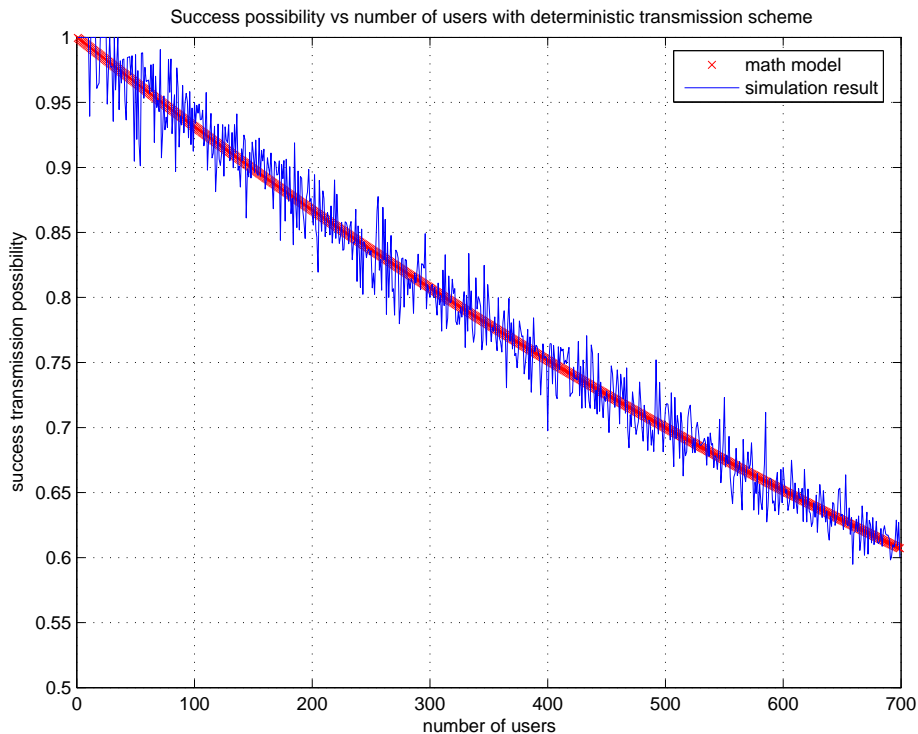


Figure 2.5: Success possibility vs number of users with deterministic transmission scheme

If we use the standard channel number $F_{ch} = 14$ of Argos-2 for example, $p_c = 0.005/14 = 1/2800$.

If there are N active users in the footprint, we can get the success probability of a single transmission P_s , which equals the probability that all the other $N - 1$ users do not transmit in its vulnerable time using the same frequency channel.

$$\begin{aligned}
 P_s &= (1 - p_c)^{2(N-1)} \\
 &= (1 - \tau/F_{ch})^{2(N-1)}.
 \end{aligned} \tag{2.4}$$

If all devices use the deterministic transmission pattern and have the same transmission interval (for the same application), once the first attempt fails due

to collision, the following retransmission will be collided as well. In this case, $P_{\text{success}} = P_s$.

The analysis and simulation results are shown in Figure 2.5. The analysis and simulation results shown in Figures 2.5, 2.6, 2.7, 2.9 are all started from two users. To ensure that the success probability is larger than a threshold, we should limit the number of users. For instance, to ensure P_{success} to be larger than 0.65, the maximum number of active users in the same footprint is 603; to ensure P_{success} is larger than 0.95, the maximum number of active users is only 72.

2.2.2 Success Probability with Randomized Transmission Scheme

Next, we investigate the effectiveness of the randomized transmission scheme. Assume that each user transmits n times during a satellite pass. The probability of fail during a pass equals the probability of all n transmissions are failed due to collisions.

When one PTT is transmitting, we define the success probability that all the other PTTs which are sharing the same frequency will not transmit in its vulnerable time $2T_b$ as $P^{(1)}$:

$$P^{(1)} = \left(\frac{R - 2T_b}{R}\right)^{\frac{N}{F_{ch}} - 1}. \quad (2.5)$$

The collision probability of one transmission try is:

$$P_c^{(1)} = 1 - P^{(1)} = 1 - \left(\frac{R - 2T_b}{R}\right)^{\frac{N}{F_{ch}} - 1}. \quad (2.6)$$

If full random level is assumed, and all the transmissions are independent, the probability of collision with another user during a pass (i.e., all n transmissions are in collisions) is:

$$P_{\text{collision}} = (P_c^{(1)})^n = \left[1 - \left(\frac{R - 2T_b}{R}\right)^{\frac{N}{F_{ch}} - 1}\right]^n \quad (2.7)$$

The success probability of transmission in a pass is:

$$\begin{aligned} P_{\text{success}} &= 1 - P_{\text{collision}} \\ &= 1 - \left[1 - \left(\frac{R - 2T_b}{R}\right)^{\frac{N}{F_{ch}} - 1}\right]^n. \end{aligned} \quad (2.8)$$

For Eq. (2.8), we assume that the collisions in different rounds are i.i.d. The result of (2.8) can be considered as the desired operating region of the system, and the deterministic scheme gives the worst performance, which is the lower bound, as shown in Fig. 2.6.

Eq. (2.8) gives the maximum number of users that a system can accommodate for a given requirement of successful transmission rate. For example, with the requirement that successful transmission probability is 0.99, a system with 14 frequency channels, $T_b = 0.5s$ and $R = 60s$ can support a maximum number of 844 users, which is much higher than that with the deterministic transmission periods.

However, some random level of transmission intervals (for example, 10% or 20%) are required to guide the implementation. Although efforts were made to derive the relationship between the successful probability of transmission and random level, the mathematical model is still not achieved. The difficulty is how to quantify the correlation of collision events in different rounds. Instead, we use simulation to find out how random level affects the system performance in the next section.

2.2.3 Numerical Results

To verify the analysis results and investigate how the random level affects system capacity, simulation programs are written in C language (in Appendix A). The analysis and simulation results are shown in Figs. 2.6, 2.7, 2.8 and 2.9. From the figures, we can see that the analytical results meet quite well with the simulation ones. We can also find from the simulation results that the successful packet delivery

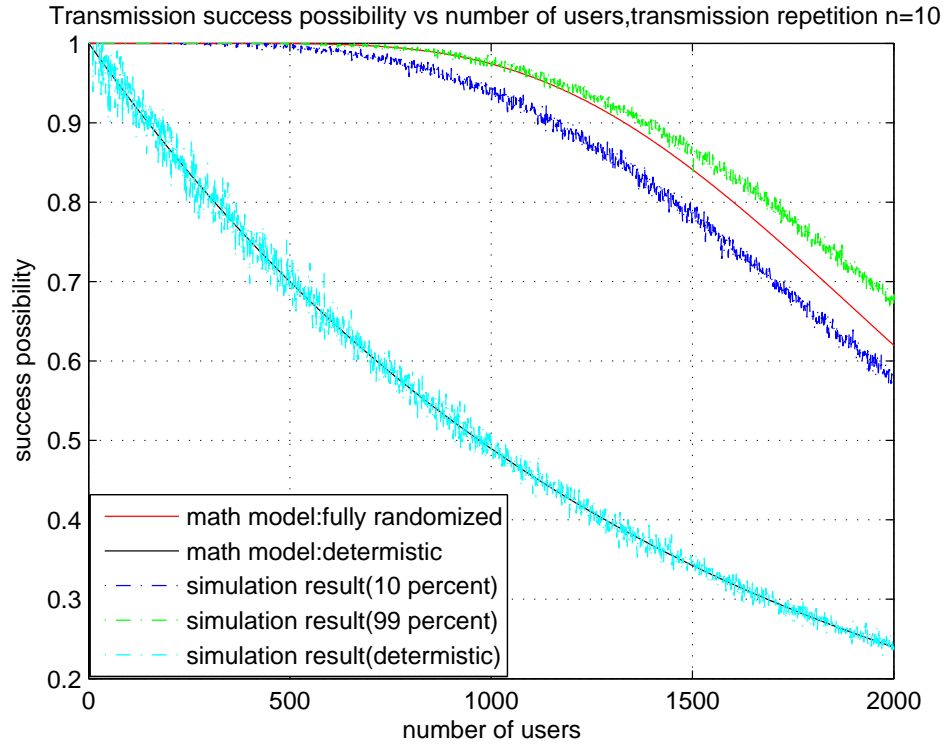
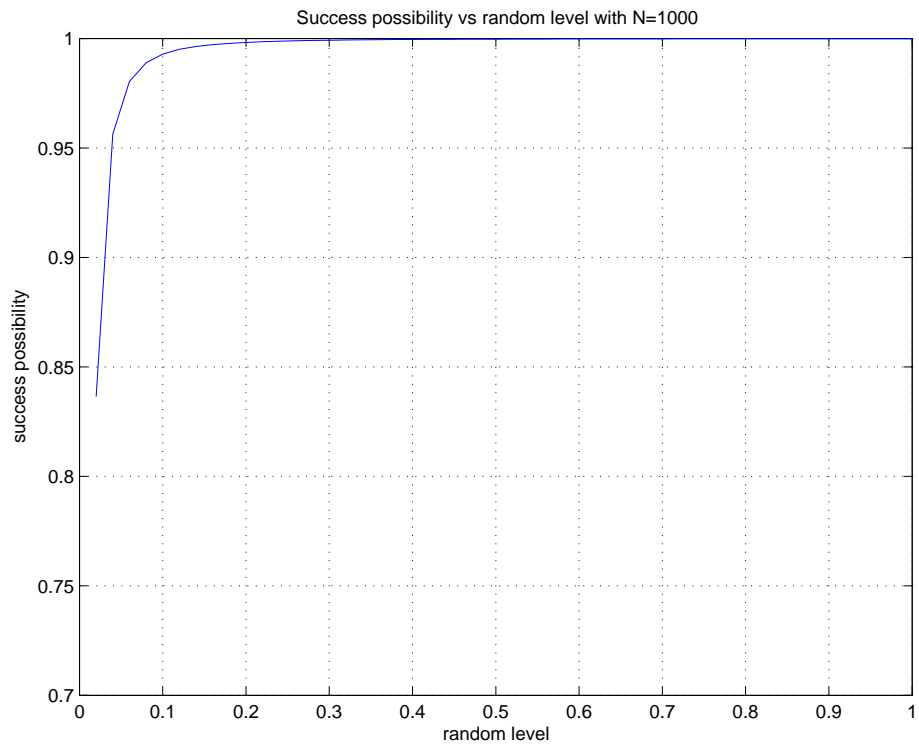


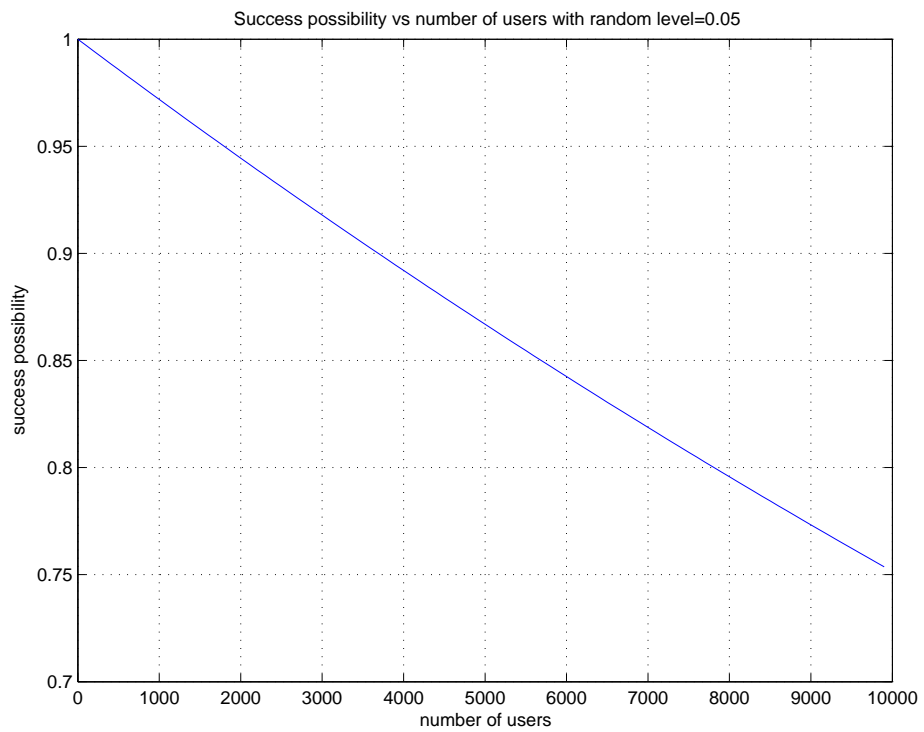
Figure 2.6: Success probability vs number of nodes

rate is not changing linearly with the random level of the transmission interval. Ten percent randomness level is good enough to improve the system performance.

From the analysis and simulation results, we also find out the relationship between the total number of users that can be supported in the same footprint and the successful reception probability of a message during a pass at different random levels. For instance, from Fig. 2.8, if each user transmits $n = 3$ times during a pass, to ensure the success rate exceeding 0.95, we can support 1000 users in a footprint if the random level is larger than 5%. Compared to the results of using the deterministic transmission pattern, to support the same number of 1000 users in the footprint, the successful reception probability of a pass is only 0.489; or to ensure the success rate of 0.95, the maximum number of users in the footprint is only 72 for the deterministic

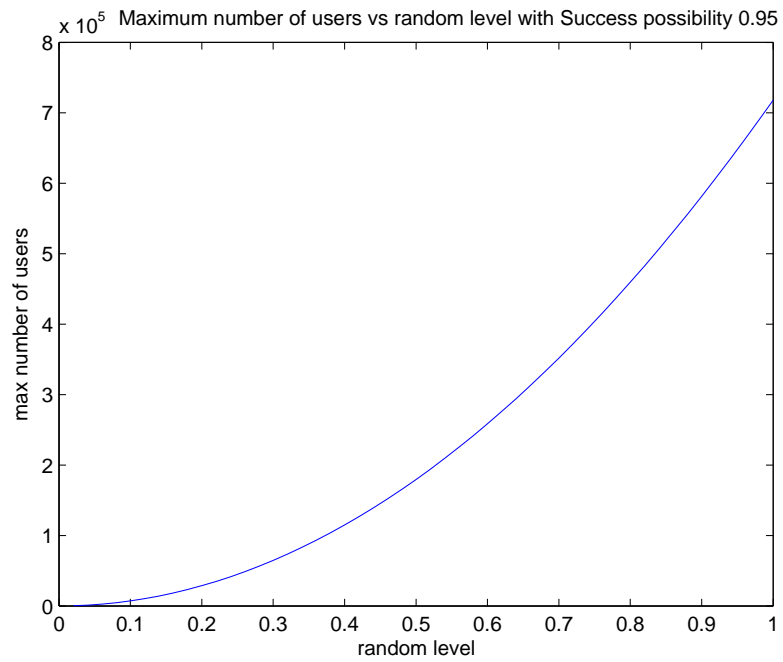


(a)

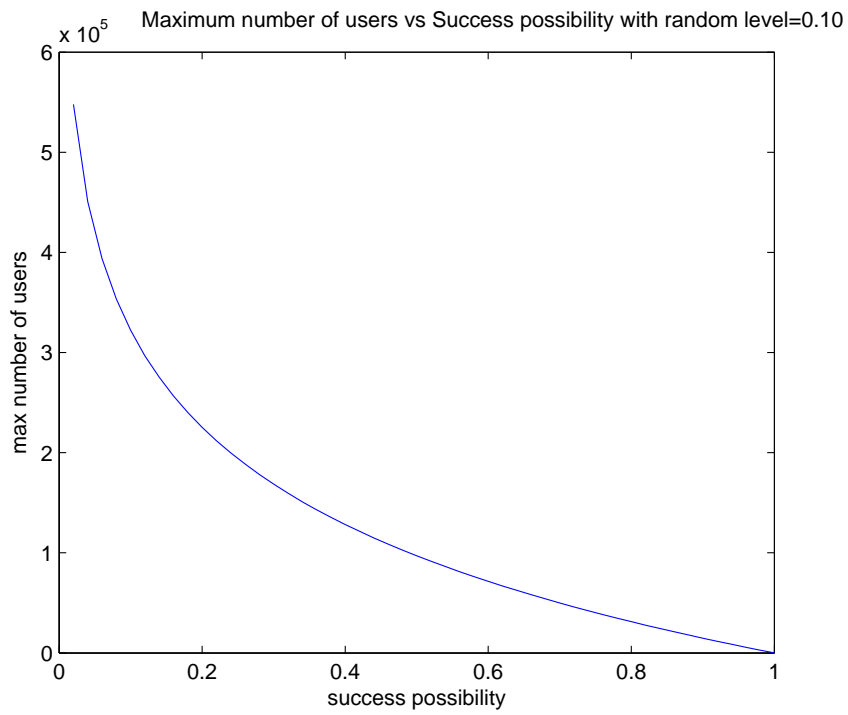


(b)

Figure 2.7: Success probability vs random level and number of user(random level 0.05)



(a)



(b)

Figure 2.8: Maximum user numbers vs random level and success probability

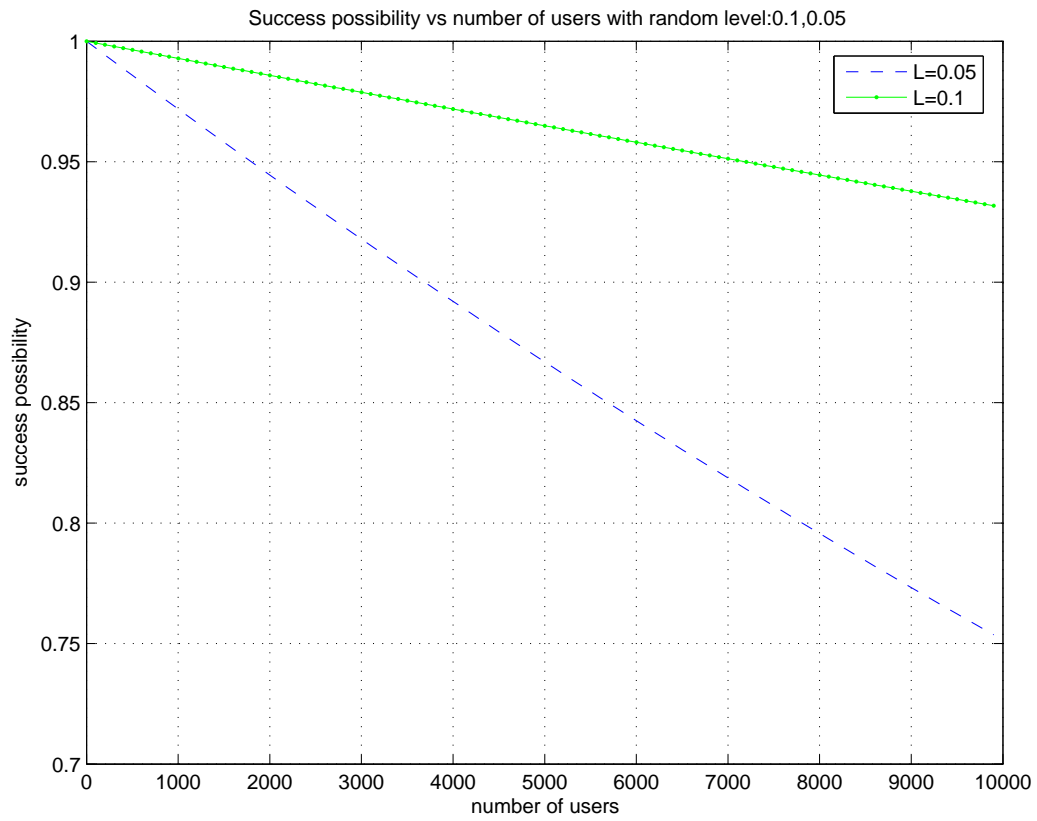


Figure 2.9: Success probability vs number of users under random level 0.1 and 0.05

case.

The relationship between the above parameters is very important for the design of the network. When we want to assure certain success reception probability in a given time interval, the number of nodes must be limited according to the curve.

2.3 Conclusion

In this chapter, we have investigated the Aloha scheme used in the Argos system. Our analysis and simulation results show that the scheme is very effective to mitigate the dead node problem. The results can be applied to other wireless sensor networks applications.

Our research results on the randomized scheme were used for bird flu monitoring, based on the phenomenon that the body temperature of infected chicken will increase by one degree Celsius. With the randomized scheme, the number of birds that can be monitored is significantly increased.

Chapter 3

Performance Analysis of TH IR-UWB with Aloha MAC Protocol

Although Impulse Radio Ultra Wideband (IR-UWB) is considered as a new technology in wireless communications, UWB actually had its origins in the spark gap transmission designed by Marconi and Hertz in the late 1890s. Due to technical limitation at that time, only one pair of transmitter-receiver was allowed in the range of the transmission [22]. As a result, narrow band technologies were preferred to UWB. However, in recent years, advances in VLSI and digital signal processing (DSP) have solved many problems that could not be addressed before. After FCC issued the Report and Order allowing its commercial deployment with a given spectral-mask requirement for both indoor and outdoor applications, UWB has attracted intensive interest both from academia and industry [1].

IR-UWB is especially well suited for short and medium range communications [23]. Its low power consumption, interference immunization, and precision localization capacities make it a promising technology for Wireless Sensor Networks. Numerous applications have been identified in health care, military and home automation [24].

The IEEE 802.15.4a standard specifies the PHY and MAC layer protocols for IR-UWB based sensor networks. It inherits the MAC strategy described in the IEEE 802.15.4 standard, but with a significant difference in the channel access strategy, due to the noise-like property of IR-UWB radio. The IR-UWB physical layer adapted in the IEEE802.15.4a standard can also supply multiple channels by burst position time hopping and pulse scrambling. In fact, Aloha was introduced as an alternative channel access strategy, based on research results of the Multi-User Interference (MUI) robustness of IR-UWB with time hopping (TH) [25]. In this and the following chapters, we will investigate the network performance of TH Aloha MAC¹ protocol together with IR-UWB, through theoretical analysis and simulation.

Since access delay with the Aloha protocol is non-significant compared to other MAC protocols, our work focuses on transmission success rate and network throughput [26]. The results are useful in designing real network applications and selecting system parameters to optimize the overall network performance.

3.1 IR-UWB Fundamentals

UWB Spectrum Mask

FCC defines UWB technology as frequency schemes that [1]

1. Either occupy a fractional bandwidth $W/f_c = 20\%$, where W is the transmission bandwidth and f_c is the center frequency, or,
2. The transmitted signal has an absolute bandwidth greater than 500 MHz.

FCC regulated spectral masks for different application categories, such as imaging, communications, and vehicular radar systems. Because this thesis deals with

¹Time hopping (TH) Aloha means that the users sharing the wireless channel using the time hopping transmission scheme and the pure Aloha random access protocol.

Table 3.1: UWB spectrum mask for indoor and outdoor data communications [1]

Frequency [MHz]	Indoor EIRP (dBm)	Indoor EIRP (dBm)
960-1610	-75.3	-75.3
1610-1990	-53.3	-63.3
1990-3100	-51.3	-61.3
3100-10600	-41.3	-41.3
≥ 10600	-51.3	-61.3

communication devices, only the spectral mask in EIRP (Equivalent Isotropically Radiated Power) limits for indoor and outdoor data applications are shown in Table 3.1. EIRP is the equivalent to the signal power level given to the antenna multiplied by the antenna gain.

IR-UWB and orthogonal frequency-division multiplexing (OFDM) UWB are two main wireless transmission schemes under the FCC regulation [24]. They are both following the FCC regulation on the bandwidth requirement, but implemented in totally different ways. In this thesis, we focus on IR-UWB scheme which is suitable for sensor networks.

IR-UWB Signaling and Modulation Techniques

The basic signaling unit of IR-UWB is impulse waveform. The pulse width is very narrow. In the IEEE 802.15.4a standard, the pulse width is approximately 2 nanoseconds, and the main lobe width is only 0.5 nanoseconds [2]. This small pulse width gives rise to a large bandwidth and a better resolution of multi-path in UWB channels.

Based on the impulse waveform, there are several modulation techniques for IR-UWB data communications, including time hopping pulse position modulation

(TH-PPM), amplitude modulation (AM), orthogonal pulse modulation (OPM), and pseudo-chaotic time-hopping (PCTH) modulation [22].

The data modulation techniques adopted in IEEE802.15.4a is time hopping impulse position modulation (TH-PPM) [2]. Data bit to be transmitted is modulated by the position of the UWB pulse. That means while bit 0 is represented by a pulse originating at the time instant 0, bit 1 is shifted in time by the amount of δ from 0, as shown in the following equation [24]:

$$x_{(t)} = W_{tr}(t - \delta d_j), \quad (3.1)$$

where W_{tr} is the impulse waveform, and d_j is the data bit with value 0, 1. The value of δ is chosen according to the autocorrelation characteristics of the pulse [24].

The IEEE802.15.4a standard uses pulse train for signaling, instead of a single pulse. Detailed discussion can be found in the following section.

3.2 IEEE802.15.4a Standard

IEEE 802.15.4a version 2007 is an amendment to IEEE 802.15.4 version 2006, specifying two additional physical layers (PHYs), UWB and Chirp Spread Spectrum (CSS). The UWB PHY specified in the standard is based upon impulse radio signaling. It is designated with 16 channels in frequency ranges: below 1 GHz, low band (3.1 and 4.8 GHz), and high band (between 6.0 and 10.6 GHz) [2]. Table 3.2 is the UWB PHY channel definition.

For UWB devices implemented in one of the three frequency band, a mandatory frequency channel must be supported. Channel 0 must be supported for devices implemented in the sub-gigahertz. Channel 3 must be supported for devices implemented in the low band. Channel 9 must be supported for devices implemented in the high band. All other remaining channels are optional.

Table 3.2: UWB PHY channel number and frequencies [2]

Channel number	Center frequency[MHz]	IR-UWB band
0	499.2	sub-gigahertz(249.6-749.6MHz)
1	3494.4	low band
2	3993.6	low band
3	4492.8	low band(mandatory)
4	3993.6	low band
5	6489.6	high band
6	6988.8	high band
7	6489.6	high band
8	7488.0	high band
9	7987.2	high band(mandatory)
10	8486.4	high band
11	7987.2	high band
12	8985.6	high band
13	9484.8	high band
14	9984.0	high band
15	9484.8	high band

In addition to the Carrier sense multiple access with collision avoidance (CSMA-CA), IEEE802.15.4a also adds Aloha for UWB channel access [2], as Aloha is a desirable choice in many sensor network applications. Because Aloha does not need clear channel assessment (CCA), the standard specifies that CCA shall always report an idle medium when Aloha channel access is adopted.

Symbol structure

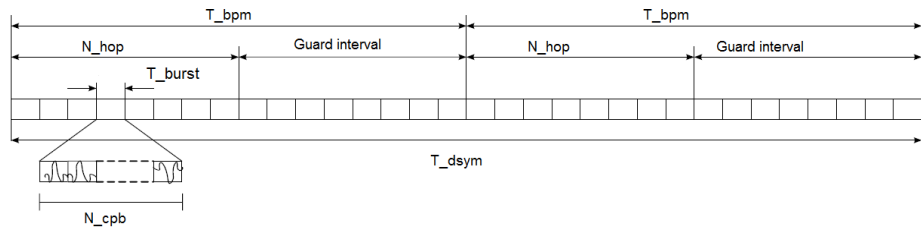


Figure 3.1: IR-UWB PHY symbol structure [2]

As defined in the IEEE802.15.4a standard, for the burst position modulation and binary phase shift keying (BPM-BPSK) modulation scheme, a UWB PHY symbol is capable of carrying two bits of information: one is used to determine the position of the burst of pulse train, while the other bit is used to modulate the burst polarity [2].

The structure of UWB symbol structure is shown in figure 3.1. The meaning of the parameters in the figure are explained as following [2].

1. Pulse width: T_c is the pulse width, or chip duration. The value of T_c is approximately 2ns;
2. Chips per burst: N_{cpb} . The value is from 1 to 512. Data rate decreases with the value of N_{cpb} .
3. Burst duration: $T_{burst} = N_{cpb} \times T_c$, from 2ns to 1025ns, is the duration of a burst;

4. Burst positions per symbol: N_{burst} . The total number of possible burst positions in a data symbol duration. The value is from 8 to 128;
5. Number of hopping positions: $N_{hop} = N_{burst}/4$, N_{burst} is the number of possible burst positions. So the burst can hop only among one-fourth of the total number of burst positions. For the mandatory mode as shown in table 3a of the standard, the number of hopping is 8 and 32;
6. Symbol duration: $T_{dsym} = N_{burst} \times T_{burst}$, from 32ns to 8205ns, see table 39a of 802.15.4a standard [2] for the values of T_{dsym} in different transmission modes;
7. Symbol rate: $R_{sym} = \frac{1}{T_{dsym}}$;
8. Mean PRF: is the average PRF (pulse repetition frequency), calculated by $Mean\ PRF = N_{cpb}/T_{dsym}$.

The bit rate of user information can be computed as:

$$Bit\ Rate = 2 \times (overall\ FEC\ rate) \times symbol\ rate. \quad (3.2)$$

The overall FEC rate is the combination of the Reed-Solomon (RS) code rate and the convolutional coding rate. The value of the overall FEC rate is either 0.44 or 0.87 [2].

Frame structure

The IR-UWB PHY frame is composed of three major components: the SHR (synchronization header) preamble, the PHR (PHY header) preamble, and the PSDU (PHY service data unit). The transmission order is SHR header first, followed by PHR, and finally the PSDU.

The standard also specifies the number of symbols in the three parts of the frame. The length of SHR preamble is from 16 to 4096 symbols. The length of PHR is always 19 symbols. Service data field can have 0 to 1209 symbols.

The value of frame transmission time depends on the mean PRF, data length, and symbol duration. The general equation to calculate the transmission interval is given in (3.3). The PHR and SHR duration can be found in table 39c in IEEE802.15.4a 2007 [2].

$$T_{frame} = T_{pre} + T_{hdr} + 16 \times Length \times T_{dsym}, \quad (3.3)$$

where “Length” is the data length in the data field in byte.

3.3 Impulse UWB Radio and Multiple User Interference

A. Impulse Radio UWB Model

The impulse radio model in our analysis follows definition in IEEE802.15.4a standard [2] and the work reported in [27] and [28]. The transmit waveform during the k_{th} symbol interval may be expressed as shown in (3.4) [2]:

$$x^{(k)}(t) = [1 - 2g_1^{(k)}] \sum_{n=1}^{N_{cpb}} [1 - 2s_{n+kN_{cpb}}] \times p(t - g_0^{(k)}T_{BPM} - h^{(k)}T_{burst} - nT_c). \quad (3.4)$$

The k_{th} symbol interval carries two information bits $g_0^{(k)}$ and $g_1^{(k)}$. Bit $g_0^{(k)}$ is encoded into the burst position, whereas bit $g_1^{(k)}$ is encoded into the burst polarity by changing $1 - 2g_1^{(k)}$ to either 1 or -1 . The sequence $s_{n+kN_{cpb}}$ is the scrambling code used during the k_{th} symbol interval, where N_{cpb} is chips per burst. $h^{(k)}$ is the k_{th} burst hopping position, and $p(t)$ is the transmitted pulse shape at the antenna input.

The signal received at the receiver is the summation of the different user's signals surrounding the radio. Assuming free-space propagation, the received signal at the receiver can be expressed as:

$$r(t) = \sum_{n=1}^{N_s} A_n x_n(t - \tau_n) + n(t), \quad (3.5)$$

where $x_n(t)$ is the transmit signal at node n , N_s is the total number of senders around the receiver, A_n is the signal attenuation from transmitter n to the receiver, $n(t)$ is white Gaussian noise, and τ_n is the signal propagation delay from node n to the receiver.

Assuming the signal from node $n = 1$ is wanted, then the received signal can be rewritten as:

$$r(t) = A_1 s_1(t - \tau_1) + \sum_{n=2}^{N_s} A_n x_n(t - \tau_n) + n(t). \quad (3.6)$$

The first part of (3.5), $A_1 s_1(t - \tau_1)$ is the signal of interest, and the second part $\sum_{n=2}^{N_s} A_n x_n(t - \tau_n)$ is called multiple user interference (MUI).

B. Scrambling and Hopping Sequence

The scrambling sequence $s_{n+kN_{cpb}}$ and the burst hopping sequence $h^{(k)}$ are generated from a common PRBS scrambler. The scrambler polynomial for the sequence generator is [2]:

$$g(D) = 1 + D^{14} + D^{15}. \quad (3.7)$$

C. Signal to Interference and Noise Ratio

Signal to Interference and Noise Ratio (SINR) is defined as the ration between the wanted signal and the cumulative interference and noise. Several factors should be

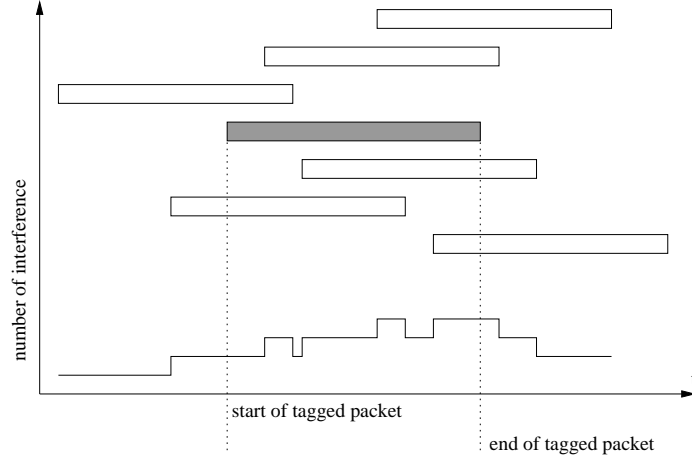


Figure 3.2: Diagram of number of interfering nodes(N_{int}) with time for Aloha

considered for evaluating the cumulative noise and interference. First is the received signal to noise ratio from the tagged packet, $\frac{E_b}{N_o}$. E_b is the average energy for transmitting a bit, and N_o is the one sided spectral density of Gaussian noise. The second factor is the interference. The number of interfering transmissions of Aloha is a time-varying parameter during the transmission of the tagged packet, as shown in Fig. 3.2. Then, processing gain G_p considers the orthogonality of the transmissions using time hopping and the time-varying scrambling sequence of the IR-UWB burst.

The SINR can be expressed as [29]:

$$\frac{E_b}{N_o + I_c} = \frac{\frac{E_b}{N_o}}{1 + \frac{N_{int} \times \frac{E_b}{N_o}}{G_p}}, \quad (3.8)$$

where I_c is the cumulative interference. $N_{int} = m - 1$, where m is the number of simultaneous transmitting nodes.

G_p is contributed from three aspects: time hopping gain G_1 , bit scrambling gain G_2 and coding gain G_3 . The total processing gain is the combination of the above factors, and it is given in (3.9). Analysis estimates the actual combination of time

hopping gain G_1 , bit scrambling gain G_2 is about 3 [30].

$$G_p = G_1 \times G_2 \times G_3 \quad (3.9)$$

D. Computation of Bit Error Probability

Bit errors are caused by the effect of white Gaussian noise and multiple user interference(MUI). The bit error probability is then can be computed with three parameters: $\frac{E_b}{N_o}$, G_p , and m , which are SNR, processing gain and the number of simultaneous transmitting nodes in the channel, respectively. The bit error probability is derived in [31] as:

$$\begin{aligned} P_b(m) = & \frac{2}{3} \times Q\left[\left(\frac{m-1}{3 \times G_p} + \frac{N_o}{2 \times E_b}\right)^{-0.5}\right] \\ & + \frac{1}{6} \times Q\left[\left(\frac{(m-1) \times G_p + \sqrt{27} \times \sigma_m}{3 \times G_p^2} + \frac{N_o}{2 \times E_b}\right)^{-0.5}\right] \\ & + \frac{1}{6} \times Q\left[\left(\frac{(m-1) \times G_p - \sqrt{27} \times \sigma_m}{3 \times G_p^2} + \frac{N_o}{2 \times E_b}\right)^{-0.5}\right], \end{aligned} \quad (3.10)$$

where $Q[\cdot]$ is the complementary error function erfc:

$$Q(x) = \frac{2}{\sqrt{\pi}} \int_x^{\infty} e^{-t^2} dt, \quad (3.11)$$

and σ_m is given by Holtzman in [31]

$$\sigma_m = m \times \left[G_p^2 \frac{23}{360} + G_p \left(\frac{1}{20} + \frac{m-1}{36} \right) - \frac{1}{20} - \frac{m-1}{36} \right]. \quad (3.12)$$

The bit error probability was further simplified in [32]:

$$P_b(m) = Q\left[\left(\frac{m-1}{3 \times G_p} + \frac{N_o}{2 \times E_b}\right)^{-0.5}\right]. \quad (3.13)$$

3.4 Related Works on UWB MAC Design and Performance Analysis

Two classes of MAC protocols have been proposed for impulse radio UWB based WPANs: distributed protocols and centralized protocols [33]. Centralized MAC protocols employ a centralized controller or access point which controls access to the medium. In this case, all nodes need to hear and talk to the controller. Centralized MAC protocols are often based on three major access techniques [11]: Frequency Division Multiple Access (FDMA) [34], Time Division Multiple Access (TDMA) [35] and Code Division Multiple Access (CDMA) [10]. FDMA assigns individual channels at different frequencies to the individual users. TDMA systems divide the radio spectrum into time slots, and in each slot only one user is allowed to either transmit or receive. In CDMA systems, a narrowband signal is multiplied by a very large bandwidth signal called the spreading signal. This spreading signal is a pseudo-noise code sequence that has a chip rate which is orders of magnitude greater than the data rate of the message. All users in the CDMA system have the same carrier frequency, but have their own pseudo-random codeword which is approximately orthogonal to all other codewords. This way, the receiver performs a time correlation operation to detect the desired codewords and all other codewords appear as noise.

A centralized approach is a good strategy for a small network with heavy traffic and strict Quality of Service (QoS) requirements. However, in large-scale ad hoc and sensor networks, the central coordination increases complexity and overheads, and it also leads to the single point of failure problem. Instead of the above MAC protocols, large scale wireless sensor networks implement distributed MAC protocols, which generally realize random access and require a method to detect medium activity. Distributed MAC protocols allow nodes to communicate without reserving

the resource through the centralized controller. One of the most widely deployed distributed wireless MAC protocols is the CSMA protocol [36]. The protocol allows any node to transmit data if it first detects an idle medium. If the medium is busy, then the node must delay its transmission until after the current transmission ends. Each individual node makes its own decision to transmit with no central guidance, so the MAC is distributed. Furthermore, the access is considered random since there is no strict order to the access.

IEEE 802.15.4 also adopts CSMA-CA as its base MAC protocol. The 802.15.4 MAC requires the following methods of CCA (clear channel assessment):

1. Detect in-band energy above threshold;
2. Detect 802.15.4-like modulation and spreading;
3. Detect 802.15.4-like modulation and spreading above threshold.

IR-UWB presents difficulties in detecting medium activity, and all three methods are difficult for systems with IR-UWB PHY layer. Actually, the low probability of detecting and intercepting a UWB signal now becomes a liability when implementing a MAC protocol for wireless sensor networks. Due to the difficulty of implementing the CSMA-CA MAC protocol, the IEEE802.15.4a standard adds Aloha as UWB channel access [2].

There are many research works on new MAC schemes and enhancement of existing narrow band MAC protocols for UWB technology. Great effort has been put on the enhancement of the existing narrowband MAC to make it better fit for the UWB, because this approach will allow for the interoperability between existing WPAN standards and UWB systems.

In 2003, the works of the Ultra Wideband concepts for Ad hoc networks (UCAN) project group [37] was funded by Information Society Technologies, follows the single

band model. UCAN MAC has considered different topologies corresponding to different applications. It also adds ranging and relaying features to IEEE 802.15.3. TDMA was chosen for channel access in intra-piconet communications. TH multiple access is used for interpiconet communications. However, the UWB features are not really exploited in UCAN, which is limited by the specifications of the IEEE 802.15.3 standard.

In 2005, Zhu et al. [38] proposed a centralized scheme inspired by the IEEE 802.15.3 standard. The scheme uses the CDMA technology to provide orthogonal channels in order to completely avoid frame collisions. In 2007, Shi et al [39] extended the work and proposed a MAC scheme for IR-UWB WPANs, which is a hybrid CDMA and TDMA approach based on time hopping spread spectrum and the timing format of IEEE 802.15.3 MAC.

N. August presented a CCA method called 'pulse sense' in 2005 [7]. The method can detect medium activity more quickly and reliably. The performance of narrowband-like CSMA-CA MAC with Pulse Sense method was also simulated and evaluated in his work.

Distributed MAC protocols for IEEE802.15.4a IR-UWB systems with CDMA and Aloha combined schemes are also well discussed in literature. In 2004, J. Boudec et al. proposed the DCC-MAC [40], which is a Decentralized MAC Protocol for 802.15.4a like UWB Mobile Ad-Hoc Networks Based on Dynamic Channel Coding. The protocol uses dynamic coding to cancel interfering energy from nearby transmitters. To solve the contention from multiple sources, the protocol uses a combination of receiver-based THSs(time hopping sequences) and invitation-based THSs. Contention for a destination uses the permanent THS depending on the receiver, but a new THS will be selected for a source-destination pair. They also built the NS2 simulation package for IR-UWB PHY, following the primitives defined in the IEEE802.15.4a standard [41].

In 2005, M. Benedetto et al. presented Aloha access protocol for IR-UWB, called $(UWB)^2$, Uncoordinated, Wireless, Baseborn medium access [42] [43]. The protocol is based on the low probability of IR-UWB pulse collision. Pure Aloha is adopted without carrier sensing. Synchronization is achieved on a frame by frame basis and a common signaling code is available for all devices in the same network for synchronization. Each transmitter has an unique code for data transmission.

In 2007, Tan et al. did some performance evaluation by analysis and simulation on slotted-Aloha over TH-UWB. Their results show that slotted-Aloha over TH-UWB has reasonable performance with the presence of multiple transmission interference [44].

To understand TH Aloha and the analytical methodologies, some works on CDMA Aloha are also reviewed. In 1981, D. Raychaudhuri published his study on the performance analysis of random access packet-switched code division multiple access systems. TH (time hopping) multiple access was analyzed under different traffic arrival models: Poisson model, Binomial model and general arrival model. He concluded that although CDMA Aloha channels degraded rapidly when loaded beyond a certain point like traditional pure Aloha and slotted Aloha, but the degradation was "more graceful" [45].

In 2000, M. Win and R. Scholtz analyzed time hopping UWB system performance. They also concluded that TH Aloha multiple access protocol performed better than traditional Aloha, and maintained stable throughput under medium and heavy load [46].

In 2007, IEEE released the IEEE 805.15.4a standard, which added IR-UWB as a optional physical layer [2]. The standard also defined the specifications of IR-UWB physical layer. Since then, a lot of works have been done on the physical layer performance analysis of IR-UWB systems specified in the standard. However, to the date of our literature review, we found very few reports on performance analysis

of MAC layer with TH Aloha. Although it is believed that TH Aloha has better performance than traditional Aloha protocol, it is not modeled according to the specifications defined in the 4a standard. This gap is our main research motivation in this thesis work. To validate our analysis, we also compare the analytical results with the simulation ones.

3.5 Performance Analysis of TH Aloha

For many sensor networks where the sensor nodes do not have receiver, pure Aloha random access protocol is probably the only choice in the MAC layer. The packet transmission process can be modeled as a Markov chain [32]. Step size of the Markov chain is the symbol time duration Δt containing two bits duration following the 802.15.4a standard. The average packet duration is \bar{T}_p . The length \bar{L} is in symbol. G is defined as the average number of generated packets of the network in the packet duration. The packet generation is assumed to be Poisson with rate λ . Every packet leaves the system with rate μ .

We denote $P_k(t)$ as the probability that there are k packets transmitting in the system at time step t . We assume that after one time step Δt , at the next symbol, the number of transmitting packets will increase by either one to be $k + 1$, or decrease by one to be $k - 1$, or remain to be k . Based on the above assumptions, we can get the steady state probability as:

$$\begin{aligned}
 P_k(t + \Delta t) &= P_k(t) \times (1 - k\mu\Delta t - \lambda\Delta t) \\
 &\quad + P_{k-1}(t) \times \lambda\Delta t \\
 &\quad + P_{k+1}(t) \times (k + 1)\mu\Delta t.
 \end{aligned} \tag{3.14}$$

We define $P(k, i)$ as the probability that the packet is transmitted successfully from first symbol to $(i - 1)_{th}$ symbol, and the number of transmitting packets is k at i_{th} symbol in the packet, as shown in Fig. 3.3.

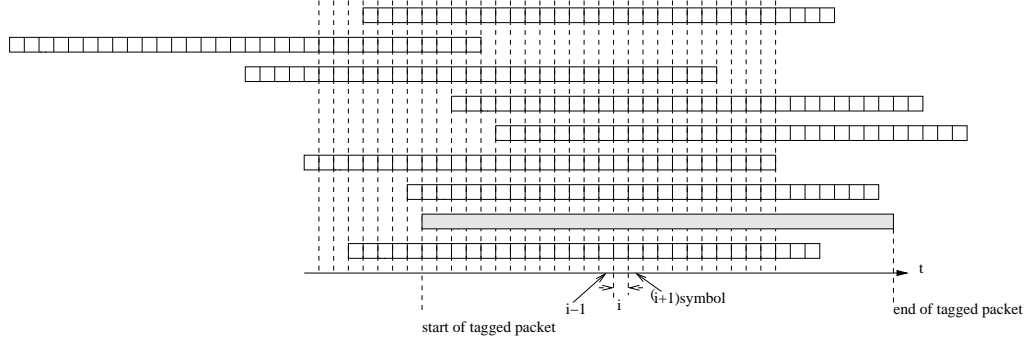


Figure 3.3: IR-UWB symbol state

At the moment that the first symbol is transmitted ($i = 1$), all the packets generated in the last \bar{T}_p time interval will be in the system. With the Poisson arrive assumption mentioned above, $P(k, i)$ at the step $i = 1$ can be expressed as:

$$P(k, i) = \frac{G^k}{k!} \exp(-G). \quad (3.15)$$

G is the average number of packets generated in an average packet time \bar{T}_p , and can be expressed as $G = \frac{\lambda}{\bar{T}_p}$.

Given the state transition probability given in (3.14) and the state bit error probability $P_b(k)$ derived in (3.13), $P(k, i)$ can be calculated recursively from the probability of previous symbol. MATLAB code for the iterative algorithm is listed below:

```
for i=2:1:L
%interference,from the first bit to the last bit
if k==1
```

```

p(k,i)=p(k,i-1)*(1-(k+1)*mu*T_b)*(1-P_b(k))
+p(k+1,i-1)*(1-P_b(k))*(k+1)*mu*T_b;
else
p(k,i)=p(k,i-1)*(1-k*mu*T_b-lambda*T_b)*(1-P_b(k-1))
+p(k+1,i-1)*(1-P_b(k+1))*(k+1)*mu*T_b+p(k-1,i-1)*(1-P_b(k-1))*lambda*T_b;
end
end

```

The packet successful probability can be expressed as:

$$P_s(L) = \sum_{k=0}^{\infty} P(k, L)(1 - P_b(k)). \quad (3.16)$$

The average throughput in a packet time is:

$$\text{Throughput} = G \times P_s(L). \quad (3.17)$$

Chapter 4

Numerical Results and Performance Evaluation by Simulation

In this chapter, we present our simulation results and compare them with the analytical results obtained in chapter 3. To simulate the TH Aloha MAC protocol, the NS2 network simulator was adopted based on the IR-UWB implementation by EPFL UWB research group [47]. We designed scenarios by setting different distance, packet size, and transmission repetition interval to evaluate the performance of TH IR-UWB networks. Network throughput and successful transmission rate for different network topology are presented and discussed.

4.1 Numerical Results of Analysis

We use one of the mandatory mode defined in the IEEE 802.15.4a standard as an example to present some theoretical analysis results of the performance of the TH Aloha system. The parameters are listed in Table 4.1 [2]. We assume that there are k simultaneously transmitting users in the system. The packet length is 128 bytes.

Table 4.1: Numerical example parameters

Parameter	Value
Bandwidth	499.2 MHz
Mean PRF	3.90MHz
FEC Rate	0.44
Burst positions per symbol N_{burst}	128
Hop positions per symbol N_{hop}	32
Chips per burst	4
Chips per symbol	512
Symbol duration	1025 ns
Symbol rate	0.98 MHz
Bit rate	0.85 Mbps

With the symbol duration of 1025 ns, the link capacity is 0.98 Mega-symbol/second, which is 1.96 Mbps if BPSK is used. Considering the coding rate of 0.44 and the preamble cost, the payload data rate will be 0.85 Mbps as shown in Table 4.1, which is the mandatory rate specified in the IEEE802.15.4a standard.

In our following results, the maximum data link frame size 128 bytes is adopted according to IEEE802.15.4a specification [2]. After the Reed Solomon(63,55) and convolution coding(0.5), the coded data field length is 2418 bits, which is 1209 symbols after modulation. Adding 64 symbols SHR and 19 symbols for PHR, the total PHY packet length is 1292 symbols. The notation “Network throughput” in Figures 4.1 and 4.2 is the amount of data from a source to a destination processed by MAC protocol divided by the total data link capacity.

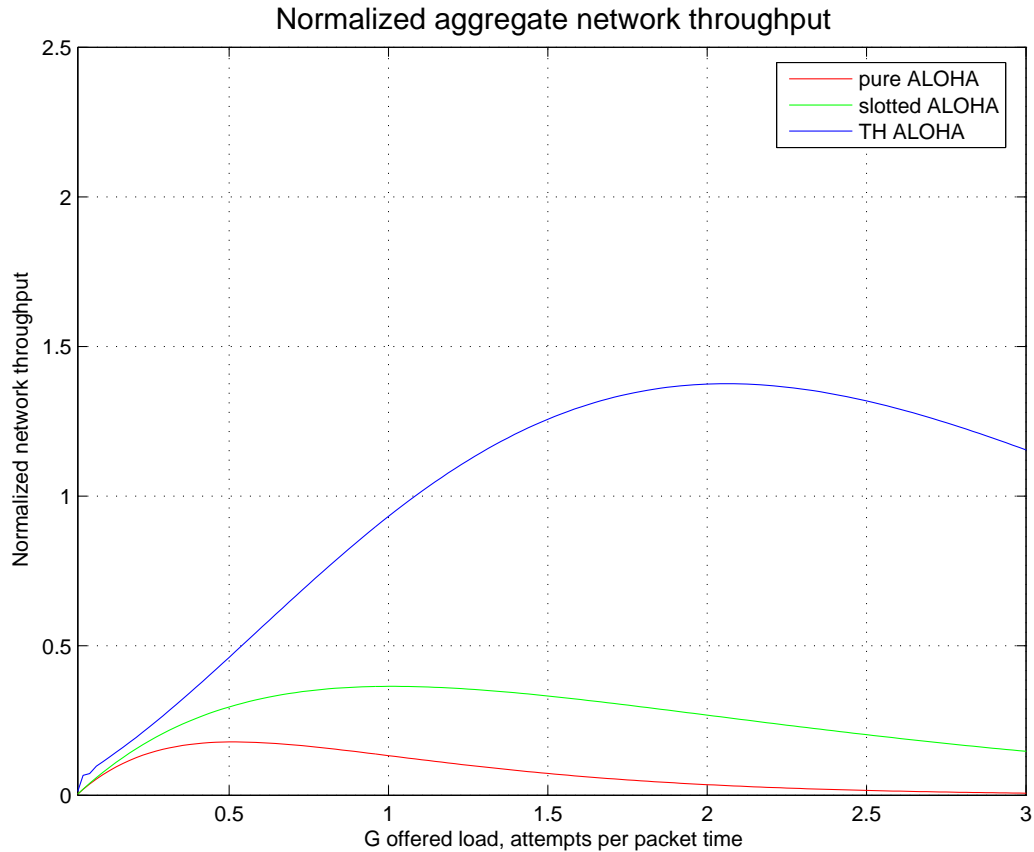


Figure 4.1: TH UWB Aloha throughput

4.1.1 Throughput vs. offered load

The throughput performance vs. the offered load is illustrated in Fig. 4.1. The throughput of pure Aloha and slotted Aloha are also presented for performance comparison, which are obtained from [6].

Because of the spread spectrum property of TH UWB, the throughput grows quickly with the offered load under light traffic. Similar to pure Aloha and slotted Aloha, the throughput of TH UWB drops when the offered load goes beyond a certain threshold, in a way more graceful compared with pure Aloha and slotted Aloha. The results also show that TH Aloha can maintain the system throughput in reasonable

level even under heavy load.

4.1.2 Impact of Packet Size on Throughput

We compare the impact of packet length on the aggregate throughput, as shown in Fig 4.2. The packet length is 32 bytes, 64 bytes, and 128 bytes respectively. We choose these small packet size as the messages in sensor networks are usually small. The results show that smaller packet size will slightly improve the aggregate throughput of the network when the traffic load is high. The reason is that given the same SNIR and BER, the packet loss rate because excessive interference of smaller packets is lower than that of larger packets.

4.2 Analysis Validation

To verify our analytical results in Chapter 3, we have done simulations with NS-2, using the similar network topology and transmission parameters compared to the analysis assumptions. Seven transmitter-receiver pairs are constructed in the simulation setting. Data link packet size is 128 bytes, which is also used in our analysis. Offered load intensity is adjusted by changing the inter-packet interval. The transmission links are lined up and separated by one meter. From the results shown in figure 4.3, our analysis agrees with the simulation quite well.

4.3 Performance Study by Simulations

In addition to the modeling and analysis, we also conduct extensive simulations with NS-2 to investigate the MAC protocol performance in various aspects. The NS-2 network simulator consists of two parts of components, one part is written in C++, implementing the basic PHY and MAC states and primitives. Modulation

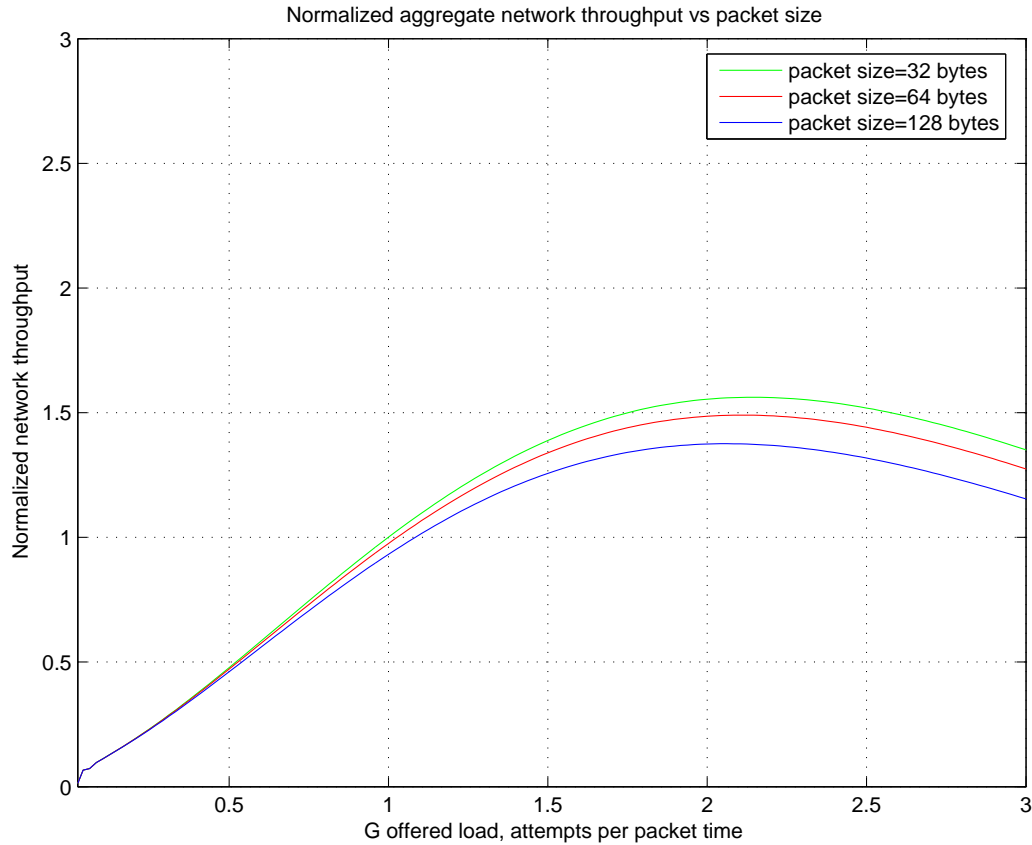


Figure 4.2: Impact of packet size on aggregate throughput

and coding are implemented in file [CodedPPM.cc]. MAC layer is implemented in file [IFControl.cc]. The second part of the components is written in TCL, which supplies the human interface to the simulator. Our simulation adopted the PHY protocol implemented by the EPFL UWB group [41].

The simulation scenario is set up by three TCL files: [scenario.tcl], [common.tcl] and [default802.15.4a.tcl]. [Scenario.tcl] defines network topology, setting up communication links by recalling procedures defined in [common.tcl]. All the default settings for PHY and MAC layers are in the TCL file [default802.15.4a]. [Common.tcl] defines the common topologies and link layer settings.

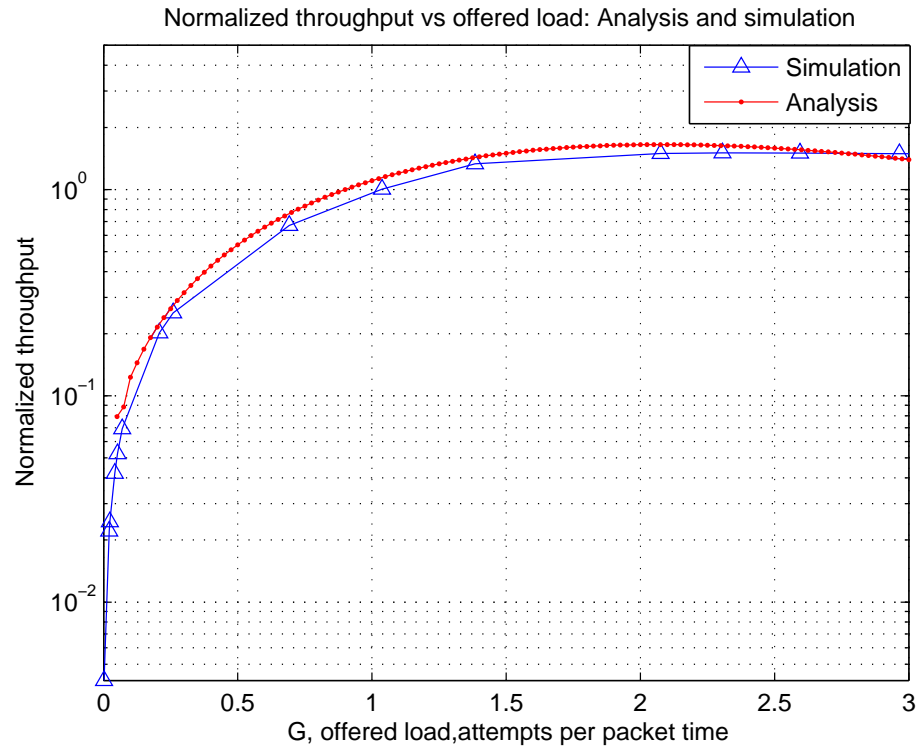


Figure 4.3: Normalized throughput vs offered load, analysis vs simulation. Packet size=128 bytes. Simulation with 7 Tx and Rx pairs, line up topology.

Simulation parameters are set in the [config] file. The parameters are explained as follows [41].

- runs: Number of runs in the simulation
- mod: Modulation scheme
- prop: Channel propagation model
- nodes: Number of nodes in the network
- distances: Area of network

Table 4.2: Simulation parameters

Parameter	Value
runs	3
Number of nodes(N)	from 2 to 30
Network area	$20m \times 20m, 40m \times 40m$
Network topology	random, symmetric
Average transmission interval	0.1s
Data packet size	32,64,128 bytes
Packet traffic model	Poisson generation process
Access strategy	pure Aloha

- preamble: Preamble time in milliseconds

The values of the parameters used in the simulations are listed in Table 4.2. The number of (active) nodes increases from 2 to 30, to cover the low density to high density network scenario. The nodes are placed in an area of $20m \times 20m$ or $40m \times 40m$. One node is set as the receiver (the data sink in the sensor networks), and all the other nodes are set as transmitters and competing for the channel. The network is loaded with $N - 1$ Constant Bit Rate (CBR) flows, where N is the total number of nodes in the network.

The link data emitting rate and aggregate data emitting rate are calculated by counting all the bits sending in one second. For example, when data link frame size is 128 bytes, and transmission interval is 0.1 s, there are 20 packets with size 2584 bits sending from the transmitter, which is 1292 symbols as calculated previously. The single data link emits data at a rate of 10.24 kbps. If there are 20 transmitting nodes in the network, the offered network load is 204.8 kbps.

We follow the network throughput definition of [48] in the following figures, which

is the amount of data from a source to a destination processed by the MAC protocol. The normalized network throughput is defined as the network throughput divided by the offered data. Simulation results are obtained by averaging the results of three simulation runs, and every simulation run lasts 200 seconds.

4.3.1 Network Performance of Symmetric Topology

Figure 4.4 presents the aggregate network throughput from our simulation results. Transmitters are symmetrically distributed on a circle with diameter 20 meters. The receiver is placed at the center of the circle. The distances from transmitters to receiver are all 10 meters. The link layer packet size is 128 bytes. There are 10 packets emitting from a single transmitter per second with inter-packet interval of 0.1 second.

The network throughput grows linearly with the number of nodes at the beginning, from 10 kbps to 130 kbps. Then, as the number of nodes increases, the aggregate throughput decreases slowly, which is far more stable than the exponential dropping of Aloha without time hopping.

Aggregate network throughput is normalized by the total offered data link load. As shown in Figure 4.5, the simulation results indicate that the performance of the network turns unstable when the data load reaches a certain point. In our simulation scenario, the successful transmission rate keeps near to one until the number of nodes exceeds 12, then drops sharply when the number of nodes increases.

Figure 4.6 shows the average delay measured in the same simulation scenario. The average delay only increases slightly from 2 ms to 3.5 ms when node number increases from 2 to 30. The increase of the delay is mainly due to the increasing load for the receiver to process.

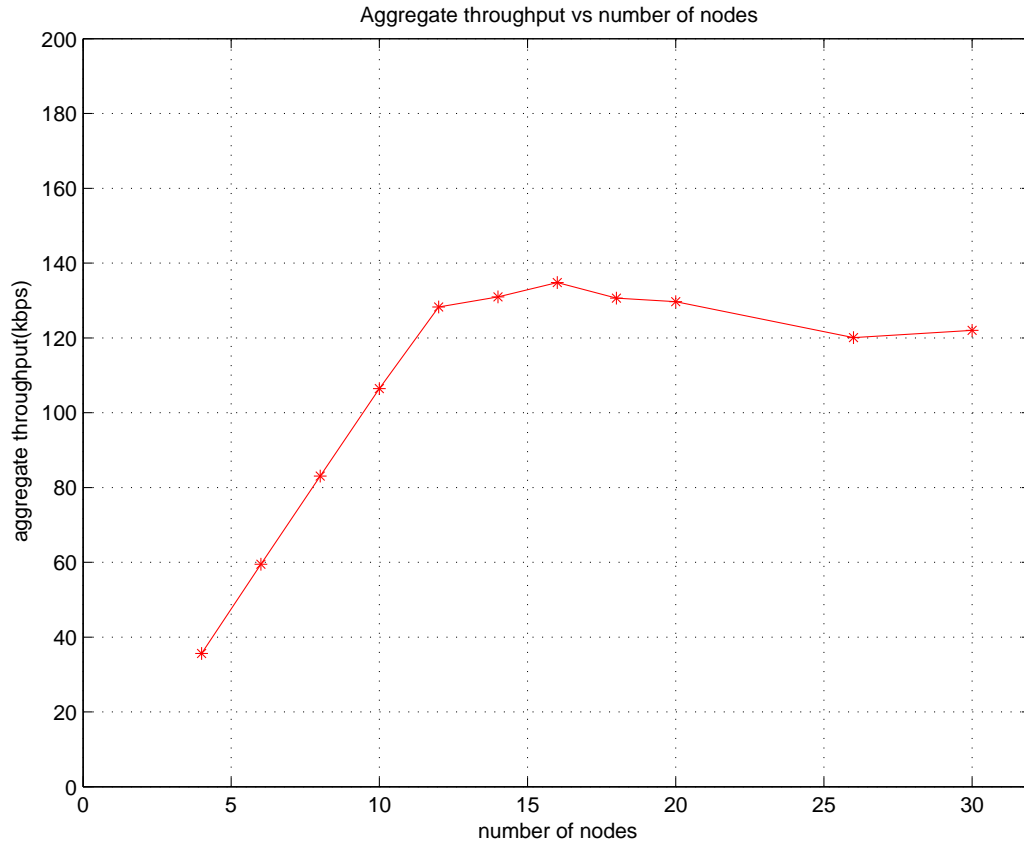


Figure 4.4: Aggregate throughput as a function of number of nodes in a symmetric topology scenario. TH Aloha, Single data link layer data rate $R= 10.2$ kbps, $20m \times 20m$ area, inter-packet interval 0.1 second)

4.3.2 Simulation of Random Topology

Figure 4.7 is the aggregate network throughput obtained from simulation under random topology. The simulation scenario is similar to the symmetric topology discussed above, except that nodes are randomly placed in an area of $20m \times 20m$. The results show that there is about 20 kbps network throughput dropping with the random topology compared to that with the symmetric topology under similar network conditions. This is mainly due to the near-far problem: when a transmitter

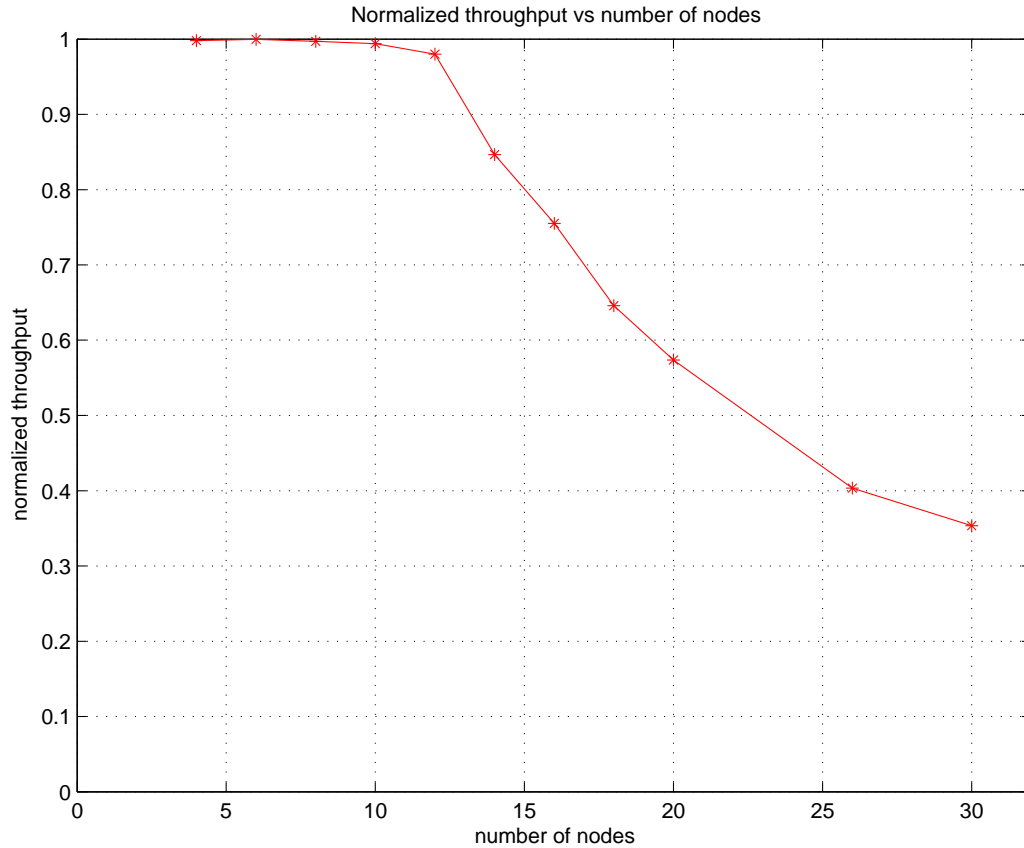


Figure 4.5: Normalized throughput vs number of nodes. Packet size=128 bytes, symmetric topology scenario. TH Aloha, Single data link layer data rate $R= 10.2$ kbps, $20m \times 20m$ area, inter-packet interval 0.1 second

near the receiver transmits, the interference to other transmissions by far-away nodes is severe.

Figure 4.8 is the comparison of the normalized network throughput between random topology and symmetric topology. The results also show that the random topology normalized network throughput drops compared to symmetric topology under similar network conditions.

Figure 4.9 is the comparison of average delay between random topology and

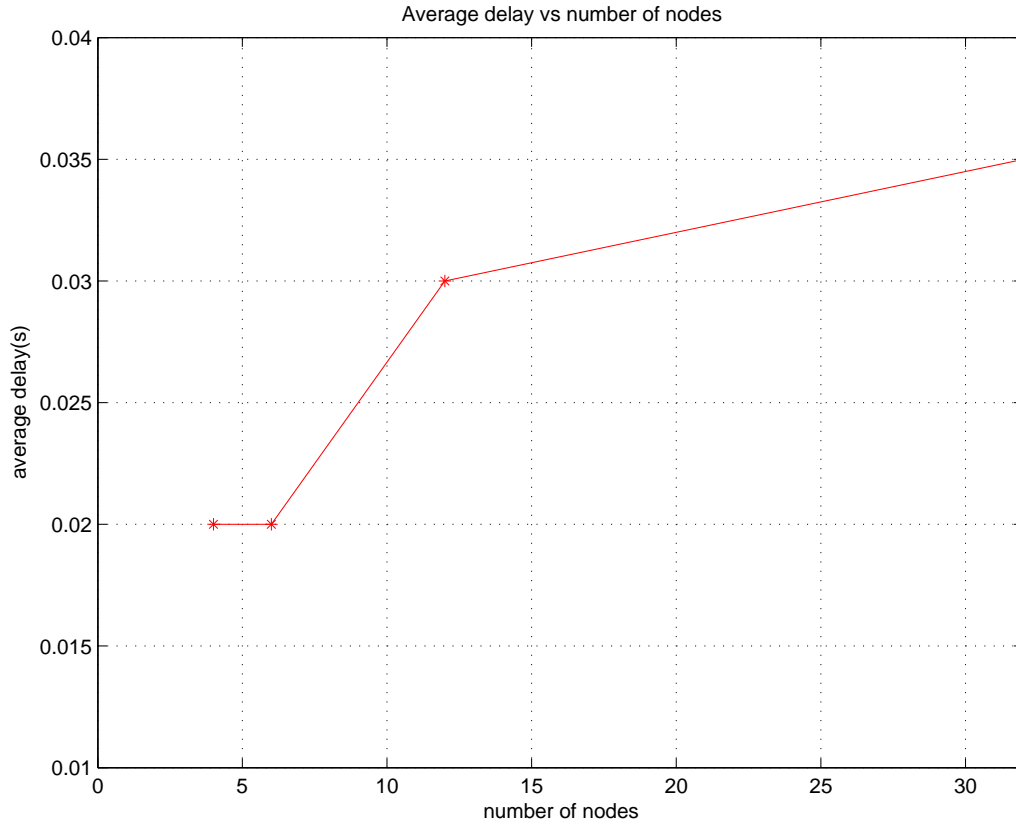


Figure 4.6: Average delay vs number of nodes. Packet size=128 bytes, symmetric topology scenario. TH Aloha, Single data link layer data rate $R= 10.2$ kbps, $20m \times 20m$ area, inter-packet interval 0.1 second

symmetric topology. Simulation log file has time stamp for every packet, both leaving transmitters and received by the receiver. Delay is measured by the difference between the two time stamp. Then average is calculated for all the packets that successfully received.

The main contribution of the delay is the receiver processing time. When node number increases, more packets will be sent to receiver, as the simulation uses a star topology. Receiver will have a longer response time than light traffic. The results show that there is no significant difference of the average delay between random topology

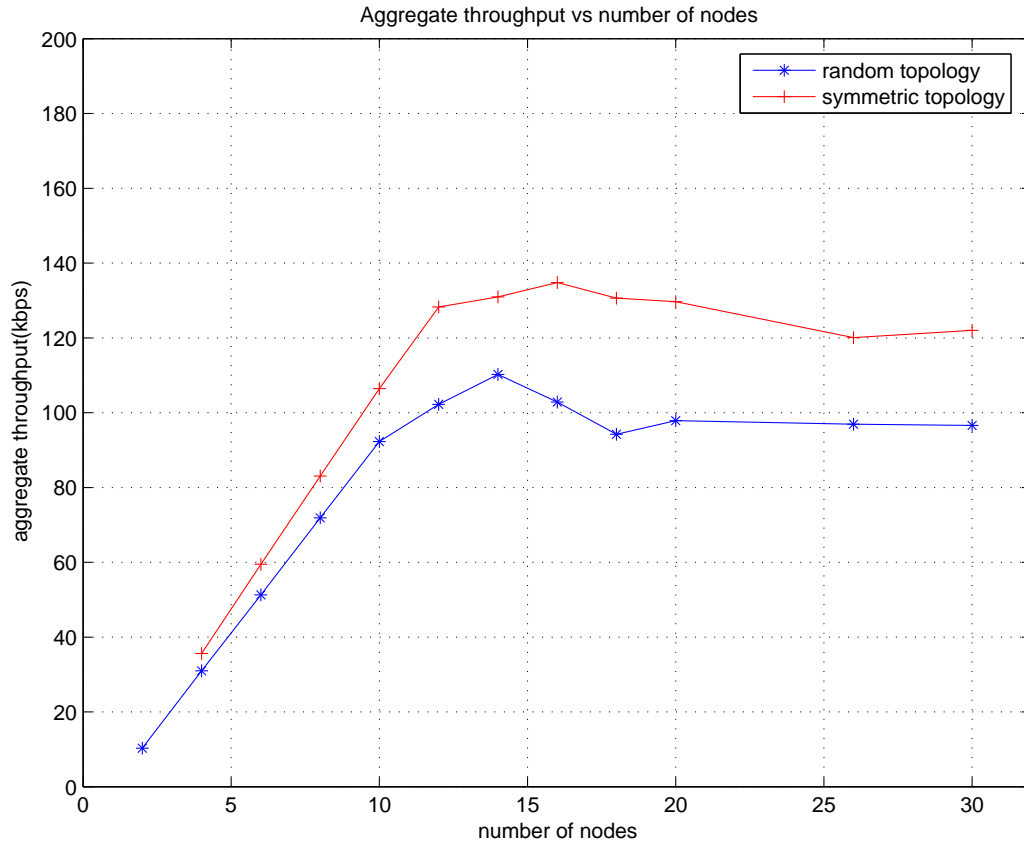


Figure 4.7: Aggregate throughput as a function of number of nodes. Random topology and symmetric topology, TH Aloha, $20m \times 20m$ area, Single data link layer data rate $R= 10.2$ kbps, inter-packet interval 0.1 second

and symmetric topology under similar network conditions.

4.3.3 Impact of Frame Size on Throughput

Figure 4.10 shows that how packet size affects the network throughput in random topology scenarios. Since average packet transmission intervals are all 0.1 second, the offered load is directly controlled by the size of data link layer frames. The single flow load is respectively 2.56 kbps, 5.12 kbps and 10.2 kbps with frame size 32 bytes,

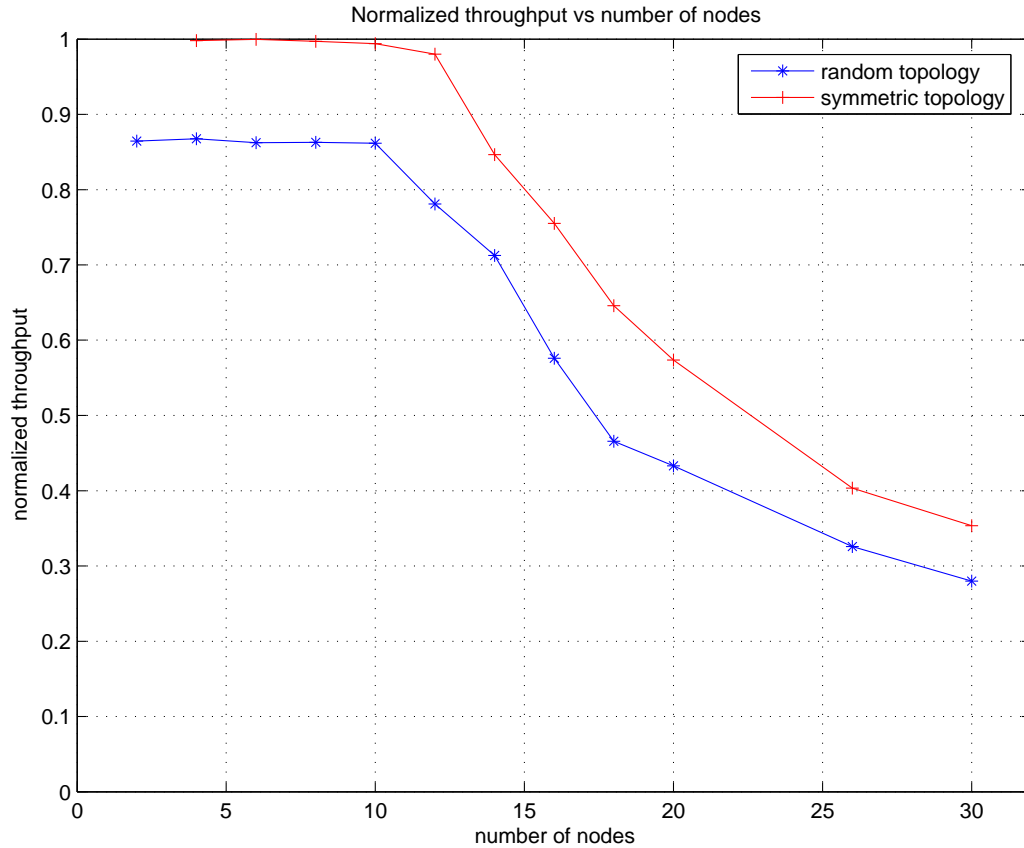


Figure 4.8: Normalized throughput vs number of nodes. Random topology and symmetric topology, TH Aloha, $20m \times 20m$ area, Single data link layer data rate $R= 10.2$ kbps, inter-packet interval 0.1 second

64 bytes and 128 bytes. Through the simulation results, we find that bigger packet size will suffer more unrecoverable packet collisions under medium and heavy load. The bigger packet size also leads to worse performance.

The above result shows that there is a tradeoff between packet size, average transmission interval and number of nodes to achieve optimized network throughput. Our results reveal that smaller packet size is more favorable to construct scalable sensor networks, as performance remains stable and reasonable at most of the regions.

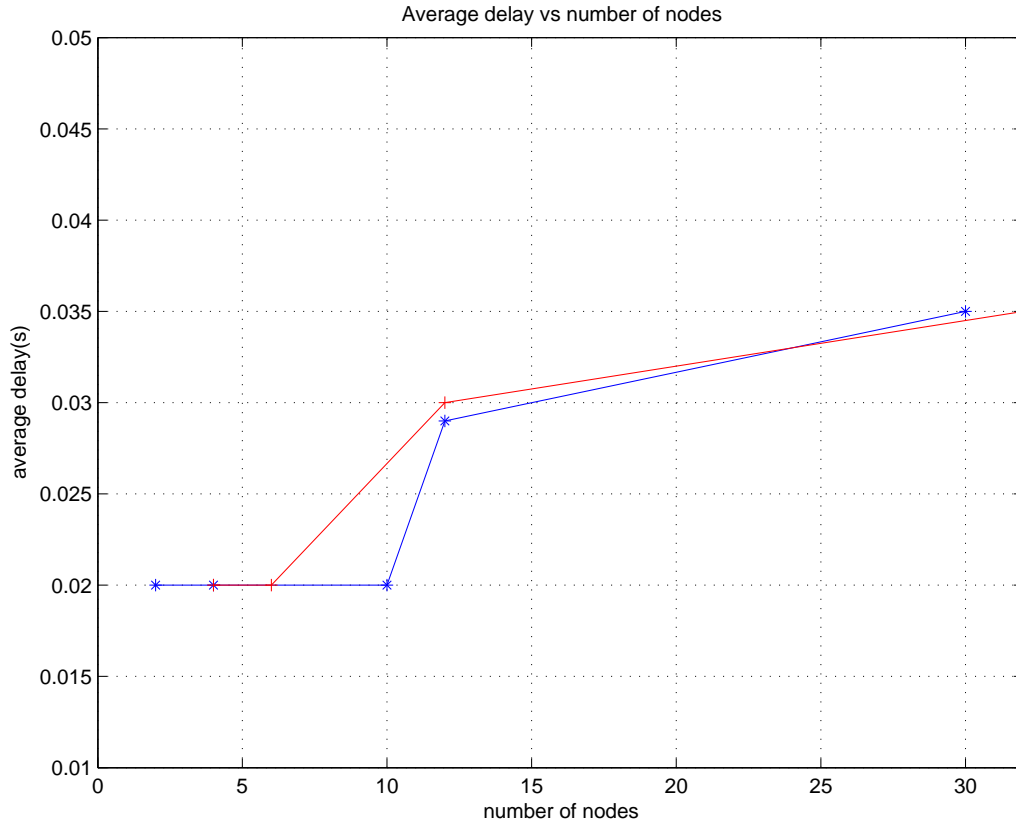


Figure 4.9: Average delay vs number of nodes. Random topology and symmetric topology, TH Aloha, $20m \times 20m$ area, Single data link layer data rate $R= 10.2$ kbps, inter-packet interval 0.1 second

4.3.4 Impact of Node Density on Network Throughput

We further investigate how the node density affects the network performance by simulation. Interference will increase with the increase of density of nodes, while other network parameters keep unchanged. On the other hand, high node density will also shorten the distance between the transmitters and receiver, which will improve the signal quality.

Figure 4.11 compares the aggregate network throughput vs number of nodes

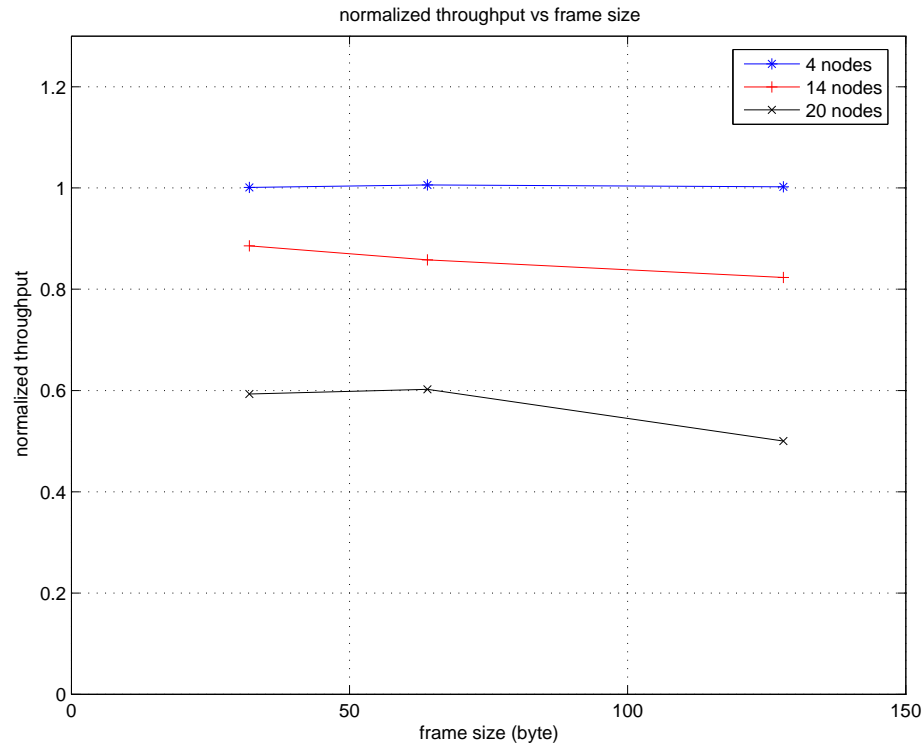


Figure 4.10: Normalized throughput affected by packet size. Random topology, TH Aloha, $20m \times 20m$ area, inter-packet interval 0.1 second

curve between network area $20meters \times 20meters$ and $40meters \times 40meters$. The figure shows that dense network has better performance because nodes are equipped with short range radio. Benefited from the collisions immunity of TH Aloha, receiver is less sensitive to interference generated from collisions between nodes.

4.3.5 Successful Packet Delivery Rate

Another important metric in sensor network design is successful packet delivery rate, which is the average number of successfully transmitted data out of the total emitted data. Different application has different requirement on successful packet delivery rate. For example, packet delivery rate is less critical in temperature and

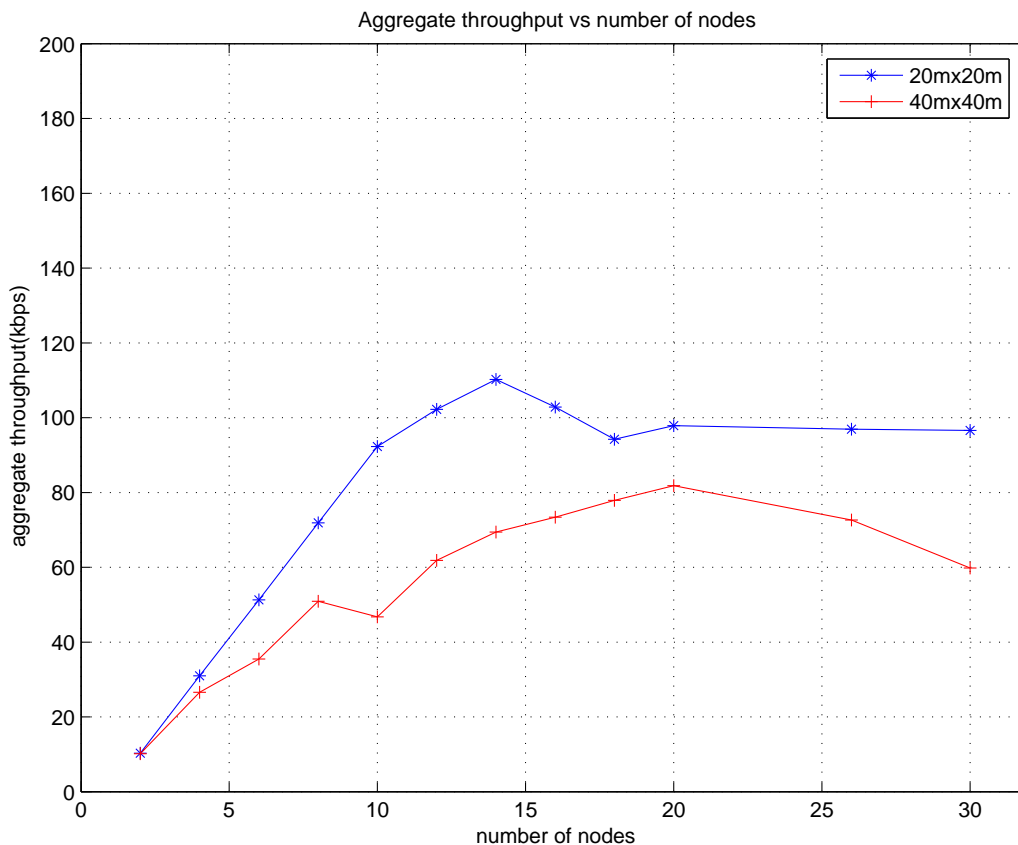


Figure 4.11: Aggregate network throughput affected by nodes density. Random topology and symmetric topology, TH Aloha, $20m \times 20m$ and $40m \times 40m$ area, Single data link layer data rate $R= 10.2$ kbps, inter-packet interval 0.1 second

pressure sensing applications than motion detection applications. Packet delivery rate requirement is also useful for choosing other parameters, such as number of nodes, average transmission interval, to balance performance of network.

Figure 4.12 illustrates the TH Aloha successful packet delivery rate under different packet size from our simulation results. The figure first shows networks with smaller packet size has better chance of successful packet delivery. It also shows that network performance drops quickly when load reach a certain point, which is 10

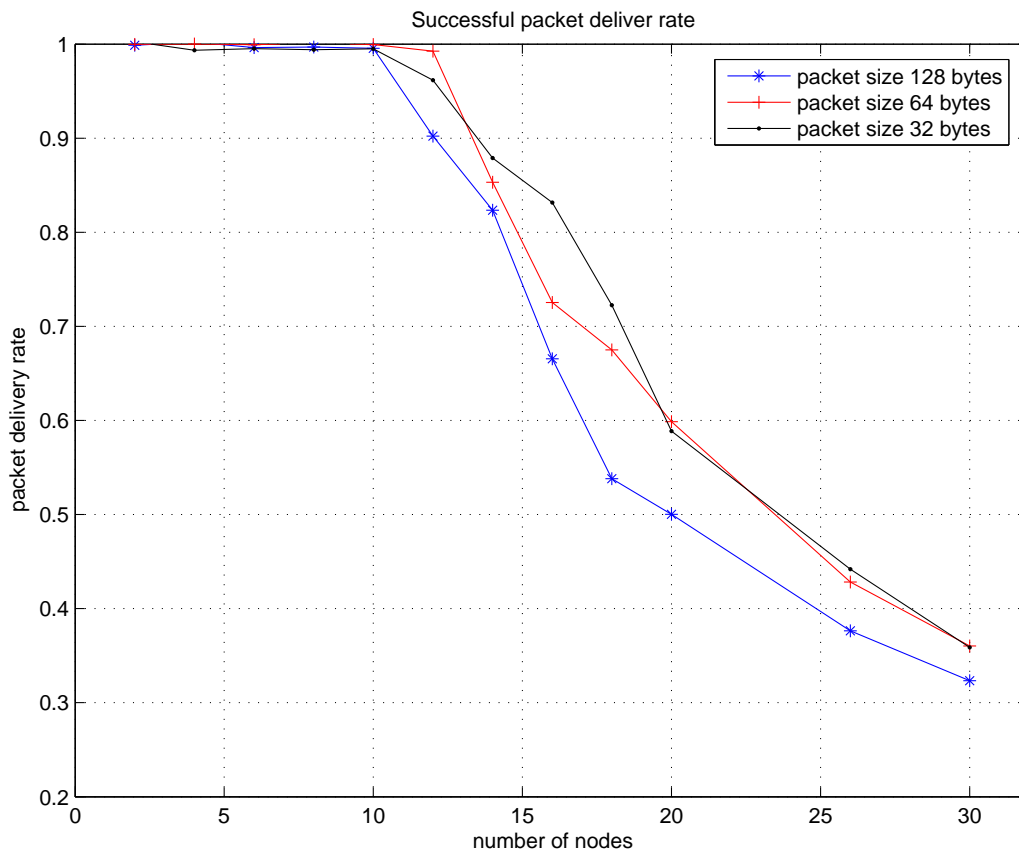


Figure 4.12: Successful packet delivery rate. Nodes are randomly placed in an area $20m \times 20m$, average transmission interval is 0.1 seconds)

to 12 nodes under our simulation conditions.

Chapter 5

Conclusion and future work

5.1 Conclusions and Summary of Contributions

In this thesis, we have studied the design and performance evaluation of several MAC protocols of wireless sensor networks. Our research focuses on the multiple access problems from different systems: ARGOS satellite telemetry system and IR-UWB system following the IEEE802.15.4a specifications. We first formulated the ARGOS system multi-user collision problem, which is from industry. The reason that resulting the long period disfunctional of sensor nodes in the same satellite footprint was that their transmissions are always synchronized with each other. To solve the problem, the randomized scheme has been proposed. Our analysis and simulation results proved that the randomized scheme can solve the dead nodes problem and also improve the overall probability of successful transmission.

The proposed randomized scheme is also demonstrated in real wireless sensor network design. The scheme was adopted and implemented in the bird flu monitoring project in early 2008. Sensor nodes are put on the bodies of chicken. Temperatures are sent back periodically to the control center. The project shows that our scheme avoided the dead nodes problem and the performance of the system was satisfied.

Realizing the importance and effect of multiple access protocols, we further extended our research to the IR-UWB system specified in the IEEE802.15.4a standard. We studied the performance of pure ALOHA protocol upon IR-UWB PHY with time hopping and compared with that of traditional narrow band ALOHA protocols. Our analysis and simulation show that, despite its simplicity, ALOHA protocol performs quite well with TH IR-UWB physical layer under light and medium load, and simultaneous transmission are possible with the IR-UWB technology.

5.2 Limitations and Further Work

There are still some issues about the randomized scheme for AOGOS system that need further study. One issue is the quantitative and control of the successful transmission probability. Our randomized scheme does not avoid collisions between nodes, and only ensure the successful transmission probability in a specific time period. In some wireless sensor applications, it is critical to receive information from certain sensor nodes with limited time delay. How to ensure certain successful transmission probability and control it by setting different repetition rate for different node is still a future work for our research on the randomized scheme.

Another issue about ARGOS randomized scheme is that reverse transmission will be enabled in the third generation ARGOS system [19]. Receivers on board of satellite will be sent back an ACK to PTT after a message is successfully received. It still needs further investigation about the performance of the randomized scheme under ARGOS 3 environment.

We did not consider the propagation channel models proposed by IEEE802.15.4a Task Group in our analysis of the performance of IEEE802.15.4a IR-UWB. We only derived the equation for throughput performance. The delay performance was not discussed in our analysis. These should be further explored. Propagation channel

models proposed by IEEE802.15.4a Task Group [49] were not adopted in the NS2 UWB PHY implementation yet. The different effects resulted from various channel models also need to be investigated.

Bibliography

- [1] “Revision of part 15 of the commissions rules regarding ultra-wideband transmission systems,” *Federal Communications Commission*, [http://www.fcc.gov/Bureaus/Engineering Technology/Orders/2002/fcc02048.pdf](http://www.fcc.gov/Bureaus/Engineering_Technology/Orders/2002/fcc02048.pdf), April 2002.
- [2] “Wireless medium access control MAC and physical layer PHY specification for low -rate wireless personal area networks LR-WPANs,” <http://www.ieee802.org/15/pub/TG4a.html>.
- [3] “Avian backpack vhf gps ptt solar transmitter,” *Habit Research*, <http://habitresearch.blogspot.com/2006/06/avian-ptt-packpack-01.html>, 2007.
- [4] “Environmental protection agency: Global earth observation system of systems (geoss),” *EPA, U.S.*, <http://www.epa.gov/geoss/>, 2006.
- [5] A. Mainwaring, D. Culler, J. Polastre, R. Szewczyk, and J. Anderson, “Wireless sensor networks for habitat monitoring,” in *Proceedings of the 1st ACM international Workshop on Wireless Sensor Networks and Applications, WSNA '02*. ACM, New York, NY, September 2002, pp. 88–97.
- [6] A. Tanenbaum, *Computer Networks, Fourth Edition*. Prentice Hall Publishing, 2003.

- [7] N. August, "Medium access control in impulse-based ultra wideband ad hoc and sensor networks," *Masters Thesis, Bradley Department of Electrical and Computer Engineering*, May 2005.
- [8] S. Kumar, V. Raghavan, and J. Deng, "Medium access control protocols for ad hoc wireless networks: A survey," *Elsevier Ad Hoc Networks*, vol. 4, no. 3, pp. 326–358, May 2006.
- [9] A. Chandra, V. Gummalla, and J. O. Limb, "Wireless medium access control protocols," *IEEE Commun. Surv.*, vol. 3, pp. 2–15, 2000.
- [10] A. Viterbi, *CDMA: principles of spread spectrum communication*. Addison Wesley Longman Publishing Co., 1995.
- [11] T. Rappaport, *Wireless Communications: Principles and practice*. Prentice Hall PTR, 2002.
- [12] N. Abramson, "The aloha system," in *Proceedings of AFIPS Conf. AFIPS Press, Montvale, N.J. Vol. 37*, 1970, pp. 281–285.
- [13] N. Joshi, S. Kadaba, S. Patel, and G. Sundaram, "Downlink scheduling in cdma data networks," in *Proceedings of the 6th Annual international Conference on Mobile Computing and Networking (Boston, Massachusetts, United States). MobiCom '00*, August 06-11 2000, pp. 179–190.
- [14] I. Demirkol, C. Ersoy, and F. Alagoz, "Mac protocols for wireless sensor networks: a survey," *Communications Magazine, IEEE*, vol. 44, no. 4, pp. 115–121, April 2006.
- [15] I. Akyildiz, W. Su, Y. Sankarasubramaniam, and E. Cayirci, "A survey on sensor networks," *IEEE Commun. Mag.*, vol. 40, no. 8, pp. 102–114, Aug 2002.

- [16] J. Wingenroth, "Satellite-based data telemetry and geolocation argos enhancements for the coastal ocean," *IEEE OCEANS'96*, vol. 1, pp. 272–276, Sept 1996.
- [17] *From Internet <http://www.projectlifesaver.org/site/>*, 2008.
- [18] D. D. Clark, "Overview of the argos system," *Proc. IEEE OCEANS'89*, vol. 3, pp. 934–939, September 1989.
- [19] "Argos 3 the new generation," *Argos system*, <http://www.argos-system.org>, 2006.
- [20] CLS, "Argos system," in *Intergovernmental Oceanographic Commission, 21th session, LA Jolla, CA, USA*, October 16-20 2006.
- [21] CNES, "Argos platform transmitter terminal (ptt) general specifications," *ARGOS*, 2003.
- [22] J. H. Reed, *Ultra wide band wireless communications and networks*. Wiley, 2006.
- [23] M. Z. Win and R. A. Scholtz., "Impulse radio: How it works," *IEEE Communications Letters*, vol. 2(2), pp. 36–37, February 1998.
- [24] I. Oppermann, *UWB Theory and Applications*. Wiley, 2004.
- [25] D. Nardis and L. Benedetto, "Overview of the ieee 802.15.4/4a standards for low data rate wireless personal data networks," *WPNC*, pp. 285–289, March 2007.
- [26] G. Ferrari and O. Tonguz, "Performance of ad hoc wireless networks with aloha and pr-csma mac protocol," in *Proceedings of Global Telecommunications Conference, 2003. GLOBECOM '03. IEEE, vol.5*, Dec 2003, pp. 2824–2829.
- [27] R. A. Scholtz, "Multiple access with time-hopping impulse radio," *Milcom Conf., Boston, MA, USA*, pp. 447–450, Oct 1993.

- [28] S. Shellhammer, “Estimating packet error rate caused by interference coexistence assurance methodology,” *IEEE P802.19 Coexistence TAG*, 2005.
- [29] D. Zeleke and M. Castro, “Aloha versus single code spread aloha for satellite systems,” *Vehicular Technology Conference*, vol. 4, pp. 2692–2696, June 2005.
- [30] D. Raphaeli and G. Kaplan, “Ieee802.15.4a proposal,” <http://grouper.ieee.org/groups/802/15/pub/05/>, Jan 2005.
- [31] J. M. Holtzman, “A simple, accurate method to calculate spread-spectrum multiple-access error probabilities,” *IEEE Trans. Communication*, vol. 40, pp. 1223–1230, March 1992.
- [32] T. Yamazato, T. Sato, K. Okada, M. Katayama, and A. Ogawa, “Throughput and delay analysis of ds/ssma unslotted aloha by non-perfect capture,” *Fourth IEEE International Conference on Universal Personal Communications*, p. 738 742, Nov 1995.
- [33] P. M. A. Gupta, “A survey on ultra wide band medium access control schemes,” *Elsevier ScienceDirect Computer Networks*, vol. 51, pp. 2976–2993, 2007.
- [34] P. H. Moose, “A technique for orthogonal frequency division multiplexing frequency offset correction,” *IEEE Transactions on Communications*, vol. 42, no. 10, pp. 2908–2914, October 1994.
- [35] R. Scholtz, “Multiple access with time-hopping impulse modulation,” in *Proc. of MILCOM’93*, October 1993, pp. 447–450.
- [36] *Wireless LAN Medium Access Control (MAC) and Physical Layer (PHY) Specifications*. IEEE 802 part 11, 1999.

- [37] F. Legrand, I. Bucaille, and S. Hethuin, "U.c.a.n ultra wide band system: Mac and routing protocols," *Proc. of Int. Workshop on Ultra Wideband Systems*, June 2003.
- [38] J. Zhu and A. O. Fapojuwo, "A complementary code-cdma-based mac protocol for uwb wpan system," *EURASIP Journal on Wireless Communications and Networking*, 2005.
- [39] Y. Y. N. Shi and I. G. Niemegeers, "Mac protocol design for impulse radio uwb based wpans," *Proc. 32nd IEEE Conference on Local Computer Networks*, 2007.
- [40] J. L. Boudec, R. Merz, B. Radunovic, and J. Widmer, "Dcc-mac: a decentralized mac protocol for 802.15.4a-like uwb mobile ad-hoc," *BROADNETS, USA: IEEE Computer Society, Los Alamitos, CA, USA*, vol. 4, no. 1, pp. 396–405, 2004.
- [41] M. Ruben, L. Boudec, Jean-Yves, and W. Jorg, "An architecture for wireless simulation in ns-2 applied to impulse-radio ultra-wide band networks," in *Proc. of 10th Communications and Networking Simulation Symposium, Norfolk, VA*, March 2007.
- [42] M. G. D. Benedetto, L. D. Nardis, M. Junk, and G. Giancola, " $(UWB)^2$: Uncoordinated, wireless, baseborn medium access for uwb communication networks," *MONET: Special Issue on WLAN optimization at the MAC and network levels*, vol. 5, no. 10, pp. 663–674, October 2005.
- [43] M. G. D. Benedetto, L. D. Nardis, G. Giancola, and D. Domenicali, "The aloha access $(UWB)^2$ protocol revisited for ieee802.15.4a," *ST Journal of Research*, vol. 4, no. 1, pp. 131–140, 2006.
- [44] H. Tan, R. K. Patro, M. C. Chan, P. Y. Kong, and C. K. Tham, "Performance of slotted-aloha over th-uwb," in *Proc. of ICUWB'07*, Sept 2007, pp. 868–873.

- [45] D. Raychaudhuri, "Performance analysis of random access packet-switched code division multiple access systems," *IEEE transactions on communications*, vol. 29, no. 6, pp. 895–900, June 1981.
- [46] M. Win and R. Scholtz, "Ultra-wide bandwidth time-hopping spread-spectrum impulse radio for wireless multiple-access communications," *IEEE transactions on communications*, vol. 48, no. 4, April 2000.
- [47] R. Merz, J. L. Boudec, and J. Widmer, "An architecture for wireless simulation in ns-2 applied to impulse-radio ultra-wide band networks," *Communications and Networking Simulation Symposium*, March 2007.
- [48] C. Perkins, "Mobile ad hoc networking terminology," *IETF Draft*, October 1997.
- [49] A. Molisch, K. Balakrishnan, and D. Cassioli, *IEEE 802.15.4a channel model - final report*. IEEE TG802.15.4a, 15-04-0662-08-004a, November, 2004.

Appendix A

ARGOS System Aloha Simulation Programs

Random.c

```
/* random.c -- Calculate the successful transmission possibility  
of Randomized Aloha scheme
```

V2.1 Dec 30,2007

Change burst to period with random bias,add matrix y[i][j]

V2.0 Oct 26,2007

Successful probability vs user number(1 to 5000);

V1.1 oct 16,2007(random.c)

- 1.Successful probability vs user number.
- 2.The random transmission simulation according to paper
- 3.Only one frequency channel is simulated.The supported user number

can be multiplied

by the actual frequency channels, since Tx are equally distributed across the channels.

V1.0 Oct 5, 2007

1. Move to gcc compiler

V0.0 Set 15, 2007

1. Time resolution is millisecond(ms)

2. Two dimensions;

3. Single frequency channel

4. Randomization level is 10 %*/

```
#include <stdio.h>
```

```
#include <math.h>
```

```
#include <time.h>
```

```
#include <stdlib.h>
```

```
main()
```

```
{
```

```
    printf("\n\n\n\n\n\n");
```

```
    printf("Simulation program for RAN-ALOHA: ");
```

```
    printf("A randomized radio transmission scheme for telemetry and sensor systems \n ");
```

```
    printf(" Simulation of multiple radio transmitters sharing the same frequency channel, calculate the successfully transmission rate for
```

```
certain number of node, repetition rate,  
    pulse width and transmission interval\n\n");  
  
printf("        Author: Haoling Ma \n");  
printf("        Copy right (2007) wireless & networking Lab, ECE,  
UVic\n\n\n");  
  
int NodeNumber,Bstwidth,Reprate,Transinterval,randomlevel,TxNumber,  
    averate,chnum;  
  
printf("How many channels are receiving(default 14)?\n");  
scanf("%d",&chnum);  
if (chnum>20) puts ("More than 20 Rx channels");  
else puts("Less than 20 Rx channels");  
  
printf("what's the transmitting pulse width in ms(default 500)?\n");  
scanf("%d",&Bstwidth);  
if (Bstwidth>1000) puts ("More than 1000ms");  
else puts("Less than 1000ms");  
  
printf("what's the repetition rate in second(default 60)?\n");  
scanf("%d",&Reprate);  
if (Reprate>100) puts ("More than 100s");  
else puts("Less than 100s");  
  
printf("what's the transmission interval in minutes(default 10  
minutes)?\n");
```

```
scanf("%d",&Transinterval);
if (Transinterval>10) puts ("More than 10mins");
else puts("Less than 10mins");

printf("what's the random level in percent(default 10)?\n");
scanf("%d",&randomlevel);
if (randomlevel>0) puts ("This is a randomized trial");
else puts("no randomization");

printf("what's the average rate(default 3)?\n");
scanf("%d",&averate);
if (averate>3) puts ("Average more than 3 times");
else puts("Average less than 3 times");

    TxNumber=(int)Transinterval*60/Reprate;
int i,j,k,m,n,s;

    FILE * pFile;
    pFile = fopen ("random.txt","w");

/* ps=1 if the node has at least one transmission doesn't overlap with
transmission from other nodes;otherwise, ps=0. avr is the average of
pt over averate */
int ps[5000],pt;

/* Percentage of successful nodes during a pass */
float p,avr;
```

```
/* Counter for no collision of a transmission. the transmission is succe
ssful if the counter is TxNumber*(NodeNumber-1) */
int nocollision;

// randomlevel=0; /*This only for norandom scheme*/

/* Transmission matrix 100x15 in the case 100 nodes, and 15 pulses */
long int t[5000][TxNumber],y[5000][TxNumber];

//groupid to nodes
int groupid[5000];

//Set random seed
srand(time(NULL));

//Tx node number change form 1 to 5000
for(n=1;n<5000;n++)
{
NodeNumber=n;
//int ps[NodeNumber];
//long int
avr=0;

//Assign groupid to nodes

for (n=0;n<NodeNumber;n++)
```

```
{
    groupid[n]=rand()%chnum;
}

//average the random
for(s=0;s<average;s++)
{

/*Initialize the arrival time of the first transmission pulse in the
transmission-node matrix */

// printf("\n ");
for(i=0;i<NodeNumber;i++)

{
t[i][0]=rand()%(Reprate*(1+randomlevel/200)*1000);
y[i][0]=t[i][0];
// printf("%ld\n ",t[i][0]);
}

/*Initialize arrival time of other transmission pulse in the transmission-node
matrix T[i,j] where i is from 0 to 99(node number=100), and j is from 1 to 15
(time interval=15mins 0 is already assigned) */

for(i=0;i<NodeNumber;i++)
{
for(j=1;j<TxNumber;j++)
```



```
if(abs(t[i][j]-t[k][m])>Bstwidth){
nocollision++;
}
}
}

else{

    //mark nocollision anyway if the groupid are not the same

for(m=0;m<TxNumber;m++)
{

nocollision++;

}
}
}

// printf("%d\n",nocollision);
if((nocollision)>=(TxNumber*NodeNumber-1)){
ps[i]=1;

// printf("%d\n",ps[i]);
}
}
}
```

```
/* calculate p(sucessful transmission percentage */

p=0;
pt=0;

for(i=0;i<NodeNumber;i++)
{
pt=pt+ps[i];
}

// printf("%d\n",pt);

avr=avr+(float)pt/averate;

} // end of average

p=avr/NodeNumber;

printf("%f  ",p);
    printf("%d users",n);

printf("\n ");
    if (pFile!=NULL)
    {
        fprintf(pFile,"%d %f\n",n,p);
```

```
    }  
  
} //end of Tx number from 1 to 5000  
  
    fclose (pFile);  
return 0;  
}
```